

Temperature-sensitive biochemical ^{18}O -fractionation and humidity-dependent attenuation factor are needed to predict $\delta^{18}\text{O}$ of cellulose from leaf water in a grassland ecosystem

Regina T. Hirl^{1,2}, Jérôme Ogée² , Ulrike Ostler^{1,3} , Rudi Schäufele¹, Juan C. Baca Cabrera¹ , Jianjun Zhu¹, Inga Schleip⁴, Lisa Wingate²  and Hans Schnyder¹ 

¹Lehrstuhl für Grünlandlehre, Technische Universität München, Alte Akademie 12, Freising-Weihenstephan 85354, Germany; ²UMR ISPA, INRAE, Villenave d'Ornon 33140, France;

³Institut für Meteorologie und Klimaforschung, Atmosphärische Umweltforschung (IMK-IFU), Karlsruher Institut für Technologie (KIT), Kreuzackbahnstraße 19, Garmisch-Partenkirchen 82467, Germany; ⁴Nachhaltige Grünlandnutzungssysteme und Grünlandökologie, Hochschule für nachhaltige Entwicklung Eberswalde, Schicklerstraße 5, Eberswalde 16225, Germany

Summary

Authors for correspondence:

Regina T. Hirl

Email: regina.hirl@tum.de

Jérôme Ogée

Email: jerome.ogee@inrae.fr

Hans Schnyder

Email: schnyder@wzw.tum.de

Received: 27 June 2020

Accepted: 18 November 2020

New Phytologist (2020)

doi: 10.1111/nph.17111

Key words: canopy conductance, grassland, isotope-enabled soil–vegetation–atmosphere transfer model (MuSICA), ^{18}O -enrichment of cellulose oxygen isotope composition of cellulose, perennial ryegrass (*Lolium perenne*), relative humidity, temperature.

- We explore here our mechanistic understanding of the environmental and physiological processes that determine the oxygen isotope composition of leaf cellulose ($\delta^{18}\text{O}_{\text{cellulose}}$) in a drought-prone, temperate grassland ecosystem.
- A new allocation-and-growth model was designed and added to an ^{18}O -enabled soil–vegetation–atmosphere transfer model (MuSICA) to predict seasonal (April–October) and multi-annual (2007–2012) variation of $\delta^{18}\text{O}_{\text{cellulose}}$ and ^{18}O -enrichment of leaf cellulose ($\Delta^{18}\text{O}_{\text{cellulose}}$) based on the Barbour–Farquhar model.
- Modelled $\delta^{18}\text{O}_{\text{cellulose}}$ agreed best with observations when integrated over *c.* 400 growing-degree-days, similar to the average leaf lifespan observed at the site. Over the integration time, air temperature ranged from 7 to 22°C and midday relative humidity from 47 to 73%. Model agreement with observations of $\delta^{18}\text{O}_{\text{cellulose}}$ ($R^2 = 0.57$) and $\Delta^{18}\text{O}_{\text{cellulose}}$ ($R^2 = 0.74$), and their negative relationship with canopy conductance, was improved significantly when both the biochemical ^{18}O -fractionation between water and substrate for cellulose synthesis (ϵ_{bio} , range 26–30‰) was temperature-sensitive, as previously reported for aquatic plants and heterotrophically grown wheat seedlings, and the proportion of oxygen in cellulose reflecting leaf water ^{18}O -enrichment ($1 - p_{\text{ex}}p_x$, range 0.23–0.63) was dependent on air relative humidity, as observed in independent controlled experiments with grasses.
- Understanding physiological information in $\delta^{18}\text{O}_{\text{cellulose}}$ requires quantitative knowledge of climatic effects on $p_{\text{ex}}p_x$ and ϵ_{bio} .

Introduction

The oxygen isotope composition of plant cellulose ($\delta^{18}\text{O}_{\text{cellulose}}$) and its enrichment above source water ($\Delta^{18}\text{O}_{\text{cellulose}}$) are thought to record environmental and physiological information of great interest to a range of scientific disciplines, including functional plant ecology and climate change biology (e.g. Barbour, 2007; Battipaglia *et al.*, 2013; Gessler *et al.*, 2014). In particular, $\delta^{18}\text{O}_{\text{cellulose}}$ or even more so $\Delta^{18}\text{O}_{\text{cellulose}}$ has been discussed as an integrated proxy of past stomatal conductance (e.g. Farquhar *et al.*, 1998; Scheidegger *et al.*, 2000; Barbour *et al.*, 2000b) that can provide information about environmental or climate change effects on the processes regulating the water-use efficiency of C_3 plants. However, empirical evidence for a direct link between $\Delta^{18}\text{O}_{\text{cellulose}}$ and stomatal conductance is currently incomplete, which prevents the use of $\delta^{18}\text{O}_{\text{cellulose}}$ time series to interpret changes in plant water use efficiency. Fundamentally, all of the

oxygen in cellulose is derived from water (DeNiro & Epstein, 1979; Liu *et al.*, 2016). Oxygen exchange with water can occur in multiple steps in the photosynthetic carbon cycle up to the formation of sucrose (or other transport sugars), and during metabolism of these sugars in sink tissues, when cellulose is being formed (Hill *et al.*, 1995; Farquhar *et al.*, 1998; Barbour *et al.*, 2005). Therefore, $\delta^{18}\text{O}_{\text{cellulose}}$ depends on the oxygen isotope composition of water in sink tissues, often approximated by the $\delta^{18}\text{O}$ of plant source water taken up by the roots ($\delta^{18}\text{O}_{\text{source}}$), and on the $\delta^{18}\text{O}$ of leaf lamina water ($\delta^{18}\text{O}_{\text{leaf}}$), respectively. During photosynthesis, leaf transpiration enriches isotopically leaf lamina water above source water ($\Delta^{18}\text{O}_{\text{leaf}} \approx \delta^{18}\text{O}_{\text{leaf}} - \delta^{18}\text{O}_{\text{source}}$). $\delta^{18}\text{O}_{\text{source}}$ can vary dynamically and is primarily controlled by the $\delta^{18}\text{O}$ of meteoric inputs ($\delta^{18}\text{O}_{\text{rain}}$; Dansgaard, 1964; Bowen & Wilkinson, 2002), their mixing with soil water and the intensity of soil evaporation (Barnes & Allison, 1988). In addition, $\delta^{18}\text{O}_{\text{source}}$ is determined by the depth distribution of

roots and their specific uptake intensities as well as by the effect of transpiration and root water uptake on soil water emptying and refilling dynamics (Brinkmann *et al.*, 2018; Hirl *et al.*, 2019).

Arguably, the oxygen isotope enrichment of cellulose above source water ($\Delta^{18}\text{O}_{\text{cellulose}} \approx \delta^{18}\text{O}_{\text{cellulose}} - \delta^{18}\text{O}_{\text{source}}$) has the most important physiological interest because of its link with $\Delta^{18}\text{O}_{\text{leaf}}$ and stomatal conductance. According to the Barbour-Farquhar model (Barbour & Farquhar, 2000),

$$\Delta^{18}\text{O}_{\text{cellulose}} = \Delta^{18}\text{O}_{\text{leaf}}(1 - p_{\text{ex}}p_x) + \epsilon_{\text{bio}}. \quad \text{Eqn 1}$$

The product $p_{\text{ex}}p_x$ reflects the proportion of oxygen in cellulose derived from source water, where p_{ex} is the proportion of exchangeable oxygen in the intermediates formed during cellulose synthesis from sucrose exported from leaves, and p_x is the proportion of source water at the site of cellulose formation. In other words, $1 - p_{\text{ex}}p_x$ represents the proportional effect of leaf lamina water ^{18}O -enrichment on the ^{18}O -enrichment of cellulose. ϵ_{bio} is the average biochemical fractionation between the organic substrate for cellulose synthesis and water (Sternberg *et al.*, 1986; Barbour, 2007).

Equation 1 relies on the assumption that $\Delta^{18}\text{O}_{\text{leaf}}$ represents the ^{18}O -enrichment of water in isotopic equilibrium with leaf sucrose, as supported by two laboratory studies on castor bean (Barbour *et al.*, 2000a; Cernusak *et al.*, 2003). In those studies, conducted in climate-controlled, steady-state conditions, the ^{18}O -enrichment of sucrose above source water ($\Delta^{18}\text{O}_{\text{sucrose}}$) was well approximated by $\Delta^{18}\text{O}_{\text{leaf}} + \epsilon_{\text{bio}}$, with ϵ_{bio} set to 27‰. However, a recent study by Lehmann *et al.* (2017) on two C_3 grass species indicated that newly formed sucrose might not always be in isotopic equilibrium with average leaf lamina water. Moreover, in submerged aquatic plants (where $\Delta^{18}\text{O}_{\text{leaf}}$ is *c.* 0) ϵ_{bio} was found to be inversely related to growth temperature, with a particularly strong temperature dependence below about 20°C (Sternberg & Ellsworth, 2011). Virtually the same temperature-sensitivity of ϵ_{bio} was found in wheat seedlings during heterotrophic growth (Sternberg & Ellsworth, 2011). Although there is a likelihood that this result applies to autotrophic terrestrial plants, it is difficult to prove because it cannot be verified, as $p_{\text{ex}}p_x$ and ϵ_{bio} cannot be measured simultaneously.

Probably, the least contentious parameter in Eqn 1 is p_x , at least in nontranspiring tissue such as the leaf-growth-and-differentiation zones of grasses or the developing cells of tree trunks, where p_x has been shown to stay close to 1 (Cernusak *et al.*, 2005; Liu *et al.*, 2017a). Sucrose is the most common carbohydrate transported within plants (Lalonde *et al.*, 2003) and the main substrate from which UDP-glucose, the immediate precursor of cellulose synthesis, is formed in heterotrophic tissue (Verbancic *et al.*, 2018), such as the leaf growth zone of grasses (Baca Cabrera *et al.*, 2020). Based on theoretical considerations of oxygen exchange between the metabolites of sucrose and water during cellulose formation and on observational data, the value of p_{ex} is often assumed to be around 0.4 (Sternberg *et al.*, 1986; Roden & Ehleringer, 1999; Barbour & Farquhar, 2000; Cernusak *et al.*, 2005), but considerable variation in p_{ex} has been suggested from

other observational studies (Gessler *et al.*, 2009; Song *et al.*, 2014; Cheesman & Cernusak, 2017). As it cannot be measured *in vivo*, estimates of p_{ex} must be obtained as a fitted parameter, whilst assuming values for p_x and ϵ_{bio} . Such estimations are sensitive to errors, including any effect of isotopic disequilibrium between $\Delta^{18}\text{O}_{\text{sucrose}}$ and $\Delta^{18}\text{O}_{\text{leaf}}$ (Lehmann *et al.*, 2017). Higher isotopic disequilibria between leaf lamina water and sucrose have also been found when air relative humidity (RH) was lower (Lehmann *et al.*, 2017). When interpreted with Eqn 1, this latter result suggests that $p_{\text{ex}}p_x$ may increase with increasing RH. A positive relationship between RH and $p_{\text{ex}}p_x$ was also suggested by the relationship between $\Delta^{18}\text{O}_{\text{cellulose}}$ and $\Delta^{18}\text{O}_{\text{leaf}}$ in the studies of Liu *et al.* (2016) and Helliker & Ehleringer (2002a) for a range of C_3 and C_4 grasses, perhaps pointing to isotopic disequilibria between $\Delta^{18}\text{O}_{\text{sucrose}}$ and $\Delta^{18}\text{O}_{\text{leaf}}$ also in these cases. Clearly, there remain important knowledge gaps on the effect of environmental conditions on ϵ_{bio} and $p_{\text{ex}}p_x$ and, hence, their implication for physiological interpretation of $\delta^{18}\text{O}_{\text{cellulose}}$ or $\Delta^{18}\text{O}_{\text{cellulose}}$ from field studies.

The temporal integration of all processes involved in the making of leaf cellulose (i.e. assimilation, mobilization of stored substrate, allocation of substrate to growth, and cellulose synthesis) represents an additional challenge when interpreting $\delta^{18}\text{O}_{\text{cellulose}}$ or $\Delta^{18}\text{O}_{\text{cellulose}}$ (Hemming *et al.*, 2001; Damesin & Lelarge, 2003; Gessler *et al.*, 2009, 2014; Royles *et al.*, 2013; Liu *et al.*, 2017b). In intensively managed grassland, shoot biomass is mostly vegetative and consists of short-lived leaves (Lemaire *et al.*, 2000). Leaf production during the growing season is continuous, with new leaf production occurring simultaneously with the senescence of older leaves (Schleip *et al.*, 2013). Accordingly, the mean live leaf age (measured in growing-degree-days (GDD)) changes relatively little during the course of the vegetation period (Lemaire *et al.*, 2000; Schleip *et al.*, 2013). In a controlled environment study with *Cleistogenes squarrosa* (a perennial C_4 grass), Liu *et al.* (2017b) found a close linear relationship between the fraction of remaining leaf elongation and the fraction of oxygen in cellulose assimilated following a change of RH in the growth environment, as inferred from ^{18}O -abundance measurements. Similar results were previously obtained by Helliker & Ehleringer (2002b), highlighting the potential of grass leaves as recorders of environmental signals in $\delta^{18}\text{O}_{\text{cellulose}}$. In light of this, allocation-and-growth models, coupled with isotope-enabled process-based models of soil-vegetation-atmosphere CO_2 and H_2O exchange, may be very useful tools for analysing the mechanisms and dynamics controlling $\Delta^{18}\text{O}_{\text{cellulose}}$ and $\delta^{18}\text{O}_{\text{cellulose}}$ in natural environments. Such models have already been applied to tree-rings (Roden *et al.*, 2000; Barbour *et al.*, 2002; Ogée *et al.*, 2009; Keel *et al.*, 2016; Lavergne *et al.*, 2017), but are presently unavailable for grassland.

The present study explores the effects of environmental drivers on the parameters of the Barbour & Farquhar (2000) model (Eqn 1), used to predict $\Delta^{18}\text{O}_{\text{cellulose}}$ and $\delta^{18}\text{O}_{\text{cellulose}}$ of leaves produced during the growing seasons of multiple years (2007–2012) in a drought-prone pasture ecosystem. Specifically, we asked the following questions: What are the effects of environmental parameters (mainly RH, temperature and soil moisture

availability) on $\Delta^{18}\text{O}_{\text{cellulose}}$ and $\delta^{18}\text{O}_{\text{cellulose}}$? Do environmentally driven adjustments of p_{ex}/p_x (RH) or ϵ_{bio} (temperature) improve predictions of observed $\Delta^{18}\text{O}_{\text{cellulose}}$ and $\delta^{18}\text{O}_{\text{cellulose}}$? Is canopy conductance reflected in $\Delta^{18}\text{O}_{\text{cellulose}}$ or $\delta^{18}\text{O}_{\text{cellulose}}$? To that end, we developed a new allocation-and-growth model suitable for grassland ecosystems (Fig. 1) that we incorporated into the ^{18}O -enabled soil–vegetation–atmosphere transfer model MuSICA. Recently, we have parameterized MuSICA for the studied pasture ecosystem and used that model to explore and predict $\delta^{18}\text{O}_{\text{source}}$ and $\delta^{18}\text{O}_{\text{leaf}}$ in that system (Hirl *et al.*, 2019). Here, we first validated the combined MuSICA and allocation-and-growth model by testing its ability to predict the labelling kinetics of autotrophic respiration observed by Gamnitzer *et al.* (2009), observed root : shoot C allocation (Schleip, 2013), and the observed $\delta^{18}\text{O}_{\text{cellulose}}$ of leaves at the study site, using integration times consistent with leaf growth dynamics observations. We then applied the model to explore the three questions developed above.

Materials and Methods

Experimental site and sampling

The study was conducted inside pasture paddock no. 8 of Grünschaige Grassland Research Station near Freising, Germany (for details on site, vegetation and grazing management see Schnyder *et al.*, 2006). Average air temperature in the study years

2007–2012 was 9.3°C, and mean annual precipitation was 753 mm (recorded at the Munich airport meteorological station). The mineral topsoil has a low water-holding capacity (66 mm plant-available field capacity) causing frequent and prolonged drought periods (Hirl *et al.*, 2019). The pasture was continuously grazed by Limousin suckler cows during the growing seasons (from mid-April to beginning of November). Animal stocking density was adjusted periodically to balance grass production and consumption by the cattle (Lemaire *et al.*, 2009), so that mean sward height was maintained at about 7 cm.

Two replicate leaf samples were collected at around midday (between 11:00 and 16:00 h Central European Summer Time) at approximately fortnightly intervals during the vegetation periods 2007–2012 (Hirl *et al.*, 2019). Each sample consisted of a mixed-species collection of the codominant species: four C_3 grasses (*Lolium perenne* L., *Poa pratensis* L., *Phleum pratense* L., *Dactylis glomerata* L.), one rosette dicot (*Taraxacum officinale* F.H. Wigg.) and one legume (*Trifolium repens* L.). The sample included only the green, nonsenescent, fully expanded leaf blades, as well as the exposed part of the growing leaf (cf. Fig. 1 of Liu *et al.*, 2017a) from 16 vegetative tillers of *L. perenne*, *P. pratensis* and *P. pratense* and two vegetative tillers of *D. glomerata*, as well as one half of a leaf blade of *T. officinale* (with the midvein removed) and two trifoliolate leaves of *T. repens*. Water in these leaf samples, along with source, soil, atmospheric humidity and rain-water samples had previously been analysed for $\delta^{18}\text{O}$, and presented and discussed in Hirl *et al.* (2019).

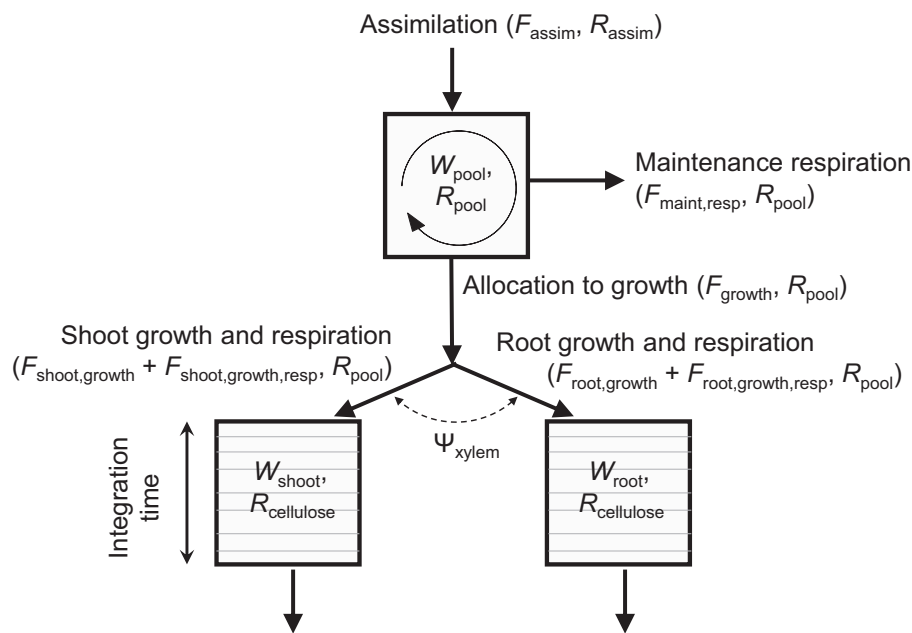


Fig. 1 Scheme of the allocation-and-growth model for predicting carbon fluxes and cellulose isotope compositions in grassland. Photosynthetic assimilation (F_{assim}) supplies substrate with specific isotopic composition (R_{assim}) to a well-mixed metabolic pool (W_{pool} , with isotope ratio R_{pool}). Maintenance respiration ($F_{\text{maint,resp}}$) and allocation of substrate to growth (F_{growth}) are both effected from the metabolic pool and thus carry the isotope signal of the pool (R_{pool}). Partitioning between shoot and root growth ($F_{\text{shoot,growth}}$ and $F_{\text{root,growth}}$, which involve growth respiration $F_{\text{growth,resp}} = F_{\text{shoot,growth,resp}} + F_{\text{root,growth,resp}}$) is governed by xylem water potential (Ψ_{xylem}). The shoot and root structural biomass pools are represented as layered (or stacked, nonmixing) pools. The integration time (d) represents the maximum age of structural leaf biomass in a sample. The size (or ‘thickness’) and isotopic composition of a given daily layer (or stack) in the shoot or root is determined by shoot and root growth rates and by the isotope ratio of the pool on that day (for details see Materials and Methods section and Supporting Information Methods S2).

Cellulose extraction and isotopic analysis

Following the procedure of Brendel *et al.* (2000) as modified by Gaudinski *et al.* (2005), α -cellulose was extracted from a subsample (50 or 25 mg) of ground plant material (for details see Liu *et al.*, 2017b). After redrying of the cellulose at 80°C for 24 h, 0.7 mg aliquots were weighed into silver cups (size: 3.3 × 5 mm, IVA Analysentechnik e.K., Meerbusch, Germany) and stored above Silica Gel orange (2–5 mm, ThoMar OHG, Lüttau, Germany) in exsiccator vessels. Samples were pyrolysed at 1400°C in a pyrolysis oven (HTO, HEKAtech, Wegberg, Germany), equipped with a helium-flushed zero blank autosampler (Costech Analytical technologies, Valencia, CA, USA), interfaced (ConFlo III, Finnigan MAT, Bremen, Germany) to a continuous-flow isotope ratio mass spectrometer (Delta Plus, Finnigan MAT). A solid internal laboratory standard (cotton powder) was included after every third or fourth sample and used for V-SMOW scaling and instrument drift correction. Every sample was analysed in duplicate. All samples and the laboratory standard were measured against a laboratory working reference carbon monoxide gas, which had previously been calibrated against a secondary isotope standard (IAEA-601; accuracy of calibration $\pm 0.25\text{‰}$ SD). The precision for the laboratory standard was $< 0.3\text{‰}$ (SD for repeated measurements). Oxygen isotope composition is expressed in per mil (‰) as $\delta^{18}\text{O} = (R_{\text{sample}}/R_{\text{standard}} - 1)$, with R_{sample} the $^{18}\text{O} : ^{16}\text{O}$ ratio of the sample and R_{standard} that in the V-SMOW standard.

Model

The integral model was composed of the ^{18}O -enabled soil–vegetation–atmosphere transfer model MuSICA (Ogée *et al.*, 2003, 2009; Wingate *et al.*, 2010; Gangi *et al.*, 2015), parameterized as in Hirl *et al.* (2019), and a new allocation-and-growth model (Fig. 1). MuSICA is a multilayer multileaf model that simulates CO_2 , water and energy redistribution and isotopic exchange processes in an ecosystem based on current mechanistic understanding (see Supporting Information Methods S1). MuSICA requires half-hourly climate data at a reference level above the vegetation (0.5 m here) as well as the isotopic composition of rainfall, CO_2 and water vapour at the same reference level. Meteorological variables were obtained from the meteorological station at Munich airport at about 3 km from the study site (wind speed, precipitation, air temperature, RH, air pressure), from two other meteorological stations at 10 and 12 km distance (radiation), and from an eddy flux station installed at the experimental site (CO_2 concentration) (Hirl *et al.*, 2019). For the precipitation and water vapour isotopic input data ($\delta^{18}\text{O}_{\text{rain}}$ and $\delta^{18}\text{O}_{\text{vapour}}$), we used data collected at the site whenever available, and gap-filled the data with offset-corrected IsoGSM data (Yoshimura *et al.*, 2011) as detailed in Hirl *et al.* (2019). $\delta^{18}\text{O}$ and $\delta^{13}\text{C}$ data of atmospheric CO_2 ($\delta^{18}\text{O}_{\text{CO}_2}$ and $\delta^{13}\text{C}_{\text{CO}_2}$) were obtained from NOAA/CMDL latitudinal products (J. Miller, pers. comm.). MuSICA parameterization included soil and vegetation properties that described the pasture system in terms of structural and hydrological characteristics, leaf gas exchange, and root

distribution and hydraulics. MuSICA, in its ‘standard parameterization’ (Hirl *et al.*, 2019), performed well in predicting $\delta^{18}\text{O}_{\text{leaf}}$, $\delta^{18}\text{O}_{\text{source}}$ (termed $\delta^{18}\text{O}_{\text{stem}}$ in Hirl *et al.*, 2019) and $\delta^{18}\text{O}_{\text{soil}}$ at different soil depths throughout seven growing seasons (2006–2012). The model also predicted the dynamics of transpiration, canopy conductance (g_{canopy}), root water uptake and plant-available soil water (PAW) (Hirl *et al.*, 2019). MuSICA parameters and parameters of the allocation-and-growth model were based on singular measurements (e.g. parameters of the soil water retention curve) or on measurements performed at intervals during the study period (e.g. canopy height, leaf area index). In the latter case, average observed values were used for the standard simulation, in agreement with the constant sward-state objective that ruled pasture management (see above). Missing parameters were taken from the literature (e.g. photosynthetic parameters) (see table S1 in Hirl *et al.*, 2019).

A detailed description of the new allocation-and-growth model (Fig. 1, Table 1) is provided in Methods S2. Briefly, the model includes three compartments: one well-mixed metabolic pool (W_{pool}) and two structural (i.e. nonmetabolic) compartments representing the aboveground shoots (W_{shoot}) and belowground roots (W_{root}), similar to Ostler *et al.* (2016). Current assimilates replenish W_{pool} with rate (F_{assim} , gross primary production) and ^{13}C and ^{18}O signatures ($\delta^{13}\text{C}_{\text{assim}}$ and $\delta^{18}\text{O}_{\text{assim}}$, see below) predicted by MuSICA (Fig. 1). Maintenance respiration ($F_{\text{maint,resp}}$) is directly supported by W_{pool} , while growth respiration ($F_{\text{growth,resp}}$) is a constant fraction of growth and included in the flux of substrate allocated to the growth of shoots and roots (F_{growth}). $F_{\text{maint,resp}}$ is an exponential function of soil surface temperature and is assumed to be proportional to total plant carbon mass and negatively related to W_{pool} when the latter decreases below a target value (Thornley & Cannell, 2000). Growth (and growth respiration) occurs only if the metabolic pool is replenished to its target value. Substrate for growth is allocated between shoot ($F_{\text{shoot,growth}}$) and root ($F_{\text{root,growth}}$) depending on root xylem water potential (Ψ_{xylem}), to account for the drought-sensitivity of leaf growth (e.g. Durand *et al.*, 1995), and the fractional allocation to the shoot ($f_{\text{shoot,growth}}$) is greater in spring than summer/autumn. New assimilates carry the isotopic signal of current assimilation, while the substrate supplied to growth and respiration carries the isotopic signal of the metabolic pool, assuming no isotopic fractionation during respiration or growth.

The $^{18}\text{O} : ^{16}\text{O}$ ratio of cellulose in a sample ($R_{\text{cellulose}}$) was calculated similar to Ogée *et al.* (2009), assuming that cellulose synthesis was proportional to shoot growth. The integration time in days was computed for a set thermal time by summing up daily mean soil temperature above a base temperature of 4°C (Schleip *et al.*, 2013). The biochemical fractionation (ϵ_{bio}) between water and substrate used in cellulose synthesis was calculated from daily mean air temperature using the empirical function found by Sternberg & Ellsworth (2011, their fig. 2). The $p_{\text{ex}}p_x$ was calculated from midday RH of air: $p_{\text{ex}}p_x = 0.016 \text{ RH} - 0.393$ (Fig. 2), derived by regressing the differences between $\Delta^{18}\text{O}_{\text{cellulose}}$ predicted with a constant, nonbiased $p_{\text{ex}}p_x$ and observed $\Delta^{18}\text{O}_{\text{cellulose}}$ against RH (Fig. 3a) as detailed in Methods S3. The resulting function closely resembled the relationship found by Lehmann

Table 1 Parameter values of the allocation-and-growth model used in Grünschwaige pasture paddock no. 8.

Parameter	Symbol	Value	Min.	Max.	Units	Comment
Total above- and belowground dry mass	DM	270	210	350	g m ⁻²	Measured
Carbon content of dry mass	C	0.43	0.42	0.46	g total C g ⁻¹ dry mass	Measured
Metabolic carbon content	w _{metab}	0.3	0.25	0.33	g metabolic C g ⁻¹ total C	Ostler <i>et al.</i> (2016)
Target metabolic pool size	W _{pool,target}	34.8	–	–	g metabolic C m ⁻² soil	Calculated from DM, C and w _{metab} (see Materials and Methods section and Supporting Information Methods S2)
Specific maintenance respiration	r _{maint,resp}	0.01	0.003	0.03	g respired C g ⁻¹ biomass C d ⁻¹	Thornley (1998)
Depth below or above the soil surface used for maintenance respiration scaling	d _{MR}	–5	–20	200	cm	
Q ₁₀ for maintenance respiration scaling	Q ₁₀	2	1	3	–	Tjoelker <i>et al.</i> (2001)
Reference temperature for maintenance respiration scaling	T _{ref}	20	15	25	°C	Lötscher <i>et al.</i> (2004)
Ψ _{xylem} -sensitivity of allocation		1	0	3		
Integration time	Δt	400	50	600	GDD	see Materials and Methods section, Fig. 4(c) and Methods S2
Maximum rate of carboxylation at 25°C	V _{cmax}	60	20	140	μmol m ⁻² s ⁻¹	Rogers <i>et al.</i> (1998)
Potential rate of electron transport at 25°C	J _{max}	100	32	224	μmol m ⁻² s ⁻¹	Calculated from V _{cmax} following Medlyn <i>et al.</i> (2002)
Slope of the Ball–Woodrow–Berry stomatal conductance model	m _{gs}	10	7	25	–	Miner <i>et al.</i> (2017), and references therein; Wohlfahrt <i>et al.</i> (1998)

'Value' denotes the parameter value used in the 'standard parameterization' and 'Min.' and 'Max.' are the minimum and maximum values used in the sensitivity analyses.

et al. (2017) (Fig. 2). Alternatively, we also calculated the isotope composition of cellulose by keeping either $p_{ex}p_x$ (0.556) or ϵ_{bio} (27‰) or both $p_{ex}p_x$ and ϵ_{bio} constant.

Statistical and sensitivity analysis

Model performance was evaluated by calculating the mean bias error (MBE = $\bar{P} - \bar{O}$, with \bar{P} the mean predicted value and \bar{O} the mean observed value) between observed and predicted $\delta^{18}\text{O}_{\text{cellulose}}$ (or $\Delta^{18}\text{O}_{\text{cellulose}}$), the mean absolute error (MAE = $\left(\sum_{j=1}^n |P_j - O_j| / n\right)$, with P_j the predicted and O_j the observed value of sample j , and n the number of samples (Willmott & Matsuura, 2005), and R^2 values. Linear regression and correlation analysis was performed to investigate the relationship between $\delta^{18}\text{O}_{\text{cellulose}}$ (or $\Delta^{18}\text{O}_{\text{cellulose}}$) and environmental parameters. All analyses were conducted in R, v.3.4.2 (R Core Team, 2017).

A sensitivity analysis was performed (1) to quantify and disentangle the effect of meteorological variables on $\Delta^{18}\text{O}_{\text{cellulose}}$ and $\delta^{18}\text{O}_{\text{cellulose}}$, and (2) to evaluate the responsiveness of $\delta^{18}\text{O}_{\text{cellulose}}$ and $\Delta^{18}\text{O}_{\text{cellulose}}$ to the parameters of the allocation-and-growth model. Two sensitivity runs were performed for each parameter or meteorological variable, using a minimum and a maximum value, based on the range of observed or expected values (see Table 1). In each sensitivity run, one parameter (or

meteorological variable) at a time was changed while all other parameters (or variables) were held the same as in the standard simulation. Regarding (1) above, the incoming short-wave radiation and wind speed, two variables that are expected to affect the leaf energy budget, were halved and doubled for each time step. Regarding (2) above, the applied parameter ranges of the allocation-and-growth model were first derived from measurements at the experimental site conducted during the study period; if no measurements were available for a parameter, relevant ranges were taken from the literature (see Table 1). Quantification of parameter effects (sensitivities) followed the procedure outlined in Hirl *et al.* (2019). First, systematic effects were quantified based on the 'mean sensitivity', computed as the mean difference between the sensitivity and the standard run $\left(\sum_{j=1}^n (\delta_{\text{sens},j} - \delta_{\text{ref},j}) / n\right)$, where $\delta_{\text{sens},j}$ is the $\delta^{18}\text{O}_{\text{cellulose},j}$ (or $\Delta^{18}\text{O}_{\text{cellulose},j}$) in a sensitivity run and $\delta_{\text{ref},j}$ is that in the standard run. Second, the variability of the parameter effect was depicted based on the standard deviation of the sensitivity, calculated from the differences between $\delta_{\text{sens},j}$ and $\delta_{\text{ref},j}$. To disentangle an eventual contribution of a temperature-sensitive ϵ_{bio} from the effects of other processes on the temperature sensitivity of $\Delta^{18}\text{O}_{\text{cellulose}}$, we also performed a range of sensitivity analyses in which air temperature was decreased (or increased) by 1, 3 or 5°C for all half-hourly values.

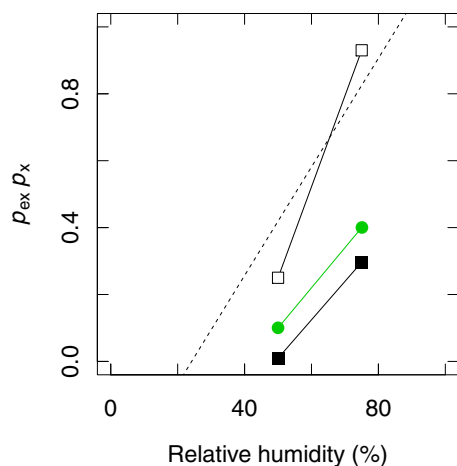


Fig. 2 Relationship between relative air humidity (RH) and $p_{ex}p_x$ from controlled environment chamber experiments with *Lolium perenne* (closed and open squares: Lehmann *et al.*, 2017; green points: J. C. Baca Cabrera *et al.* unpublished data). For both datasets, $p_{ex}p_x$ was calculated based on Eqn 1, using $\Delta^{18}\text{O}_{\text{leaf}}$ and $\Delta^{18}\text{O}_{\text{cellulose}}$ data. The biochemical fractionation (ϵ_{bio}) was computed from the temperature (T) of the chamber air according to the relationship found by Sternberg & Ellsworth (2011) for submerged aquatic plants ($\epsilon_{\text{bio}} = 0.00737T^2 - 0.4375T + 32.528$; see their Fig. 2) and yielded $\epsilon_{\text{bio}} = 26.8\text{‰}$ for the unpublished data of JCBC, RTH, JZ and HS (green points) and $\epsilon_{\text{bio}} = 25.5\text{‰}$ for the study of Lehmann *et al.* (2017) (closed squares). Open squares represent $p_{ex}p_x$ calculated by assuming $\epsilon_{\text{bio}} = 27\text{‰}$ (as reported by Lehmann *et al.*, 2017, their Table 4). RH was constant throughout day and night in the experiment of Lehmann *et al.* (2017), but differed between the dark and light period in the experiment of JCBC, RTH, JZ and HS (50%/75% and 75%/75%) (other experimental details are reported in Baca Cabrera *et al.*, 2020). The dashed line indicates the $p_{ex}p_x$ vs RH relationship used in the 'standard simulation', calculated from the relationship between model-data residuals and RH when a constant $p_{ex}p_x = 0.556$ was applied in the simulation (see Fig. 3 and Supporting Information Methods S3).

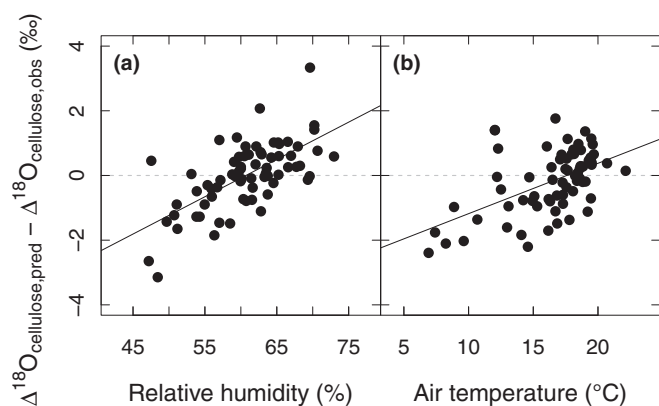


Fig. 3 Difference between predicted and observed $\Delta^{18}\text{O}_{\text{cellulose}}$ (a) in relation to relative humidity (RH), when $\Delta^{18}\text{O}_{\text{cellulose}}$ was predicted with a constant $p_{ex}p_x = 0.556$ and a temperature-dependent ϵ_{bio} (as in the 'standard simulation'), and (b) in relation to air temperature, when $\Delta^{18}\text{O}_{\text{cellulose}}$ was modelled using a constant $\epsilon_{\text{bio}} = 27\text{‰}$ and a RH-dependent $p_{ex}p_x$ (as in the 'standard simulation'). RH and air temperature represent the 400 GDD average of midday (± 3 h around noon) humidity and daily mean temperature, respectively.

Results

Metabolic pool turnover, carbon allocation and integration time

The turnover of the metabolic pool was validated by comparing the predicted ^{13}C -labelling of W_{pool} (f_{new} , the fraction of labelled C in W_{pool}), forced by a step-change of $\delta^{13}\text{C}_{\text{CO}_2}$ in the MuSICA input data, with the labelling kinetics of total autotrophic respiration observed at the same site in May 2007 (Gamnitzer *et al.*, 2009; see their fig. 5). The predicted f_{new} in W_{pool} matched closely the observed fraction of labelled C in total autotrophic respiration (slope = 0.99; intercept = 0.06; $R^2 = 0.98$; $P < 0.001$; Fig. 4a).

Model predictions for the fraction of carbon allocated to shoot growth ($f_{\text{shoot,growth}}$) compared well with observations of $f_{\text{shoot,growth}}$ made by Schleip (2013) in the same pasture during May and September of 2007. The model predicted average $f_{\text{shoot,growth}}$ of 0.67 for spring and 0.54 for autumn 2007, while Schleip (2013) observed an average carbon allocation fraction to shoot growth of 0.65 (± 0.05 SE) and 0.5 (± 0.05 SE) over the same periods (Fig. 4b). The average allocation to aboveground biomass for all spring and summer/autumn periods 2007–2012 was 0.58 and 0.47, respectively.

To constrain the integration time of the ^{18}O -signal in the leaf cellulose samples, we compared the R^2 between observed and predicted $\delta^{18}\text{O}_{\text{cellulose}}$ (Fig. 4c) for predictions of $\delta^{18}\text{O}_{\text{cellulose}}$ based on integration times of 50–600 GDD. Those calculations were made with the model in its standard parameterization (Table 1) and assumed leaf growth started on the 15 March every year. The R^2 between observed and predicted $\delta^{18}\text{O}_{\text{cellulose}}$ increased up to an integration time of 400 GDD ($R^2 = 0.57$) and decreased beyond that. This integration time of 400 GDD translated to time spans varying between 22 and 59 d in different periods, depending on thermal conditions (Fig. 4d) and was subsequently used as the standard integration time for all predictions of $\delta^{18}\text{O}_{\text{cellulose}}$ and $\Delta^{18}\text{O}_{\text{cellulose}}$.

Observed variation of $\delta^{18}\text{O}_{\text{cellulose}}$ and $\Delta^{18}\text{O}_{\text{cellulose}}$

$\delta^{18}\text{O}_{\text{cellulose}}$ displayed dynamic variation within and between years, with pronounced increases and decreases in some years (2007, 2010) and lower variability in others (2008, 2011; Fig. 5). The total range of observed $\delta^{18}\text{O}_{\text{cellulose}}$ was 5.1‰, and a clear seasonal pattern was not evident (right panel, Fig. 5a). Annual mean $\delta^{18}\text{O}_{\text{cellulose}}$ did not differ significantly between the individual years, except for 2010 when the mean was 1.5‰ lower than the average of the other years. The lower $\delta^{18}\text{O}_{\text{cellulose}}$ in 2010 was linked to a more negative $\delta^{18}\text{O}_{\text{rain}}$ and lower leaf water ^{18}O -isotopic enrichment in that year (cf. Hirl *et al.*, 2019).

The range of observed $\Delta^{18}\text{O}_{\text{cellulose}}$ was 50% greater than that of $\delta^{18}\text{O}_{\text{cellulose}}$ (compare Fig. 5a and b). Unlike $\delta^{18}\text{O}_{\text{cellulose}}$, average $\Delta^{18}\text{O}_{\text{cellulose}}$ declined distinctively during the growing season at a rate of 0.83‰ per month ($R^2 = 0.90$; $P < 0.01$). This was related to an increasing trend of $\delta^{18}\text{O}_{\text{source}}$ over the growing season (Hirl *et al.*, 2019). Overall, the observed variation

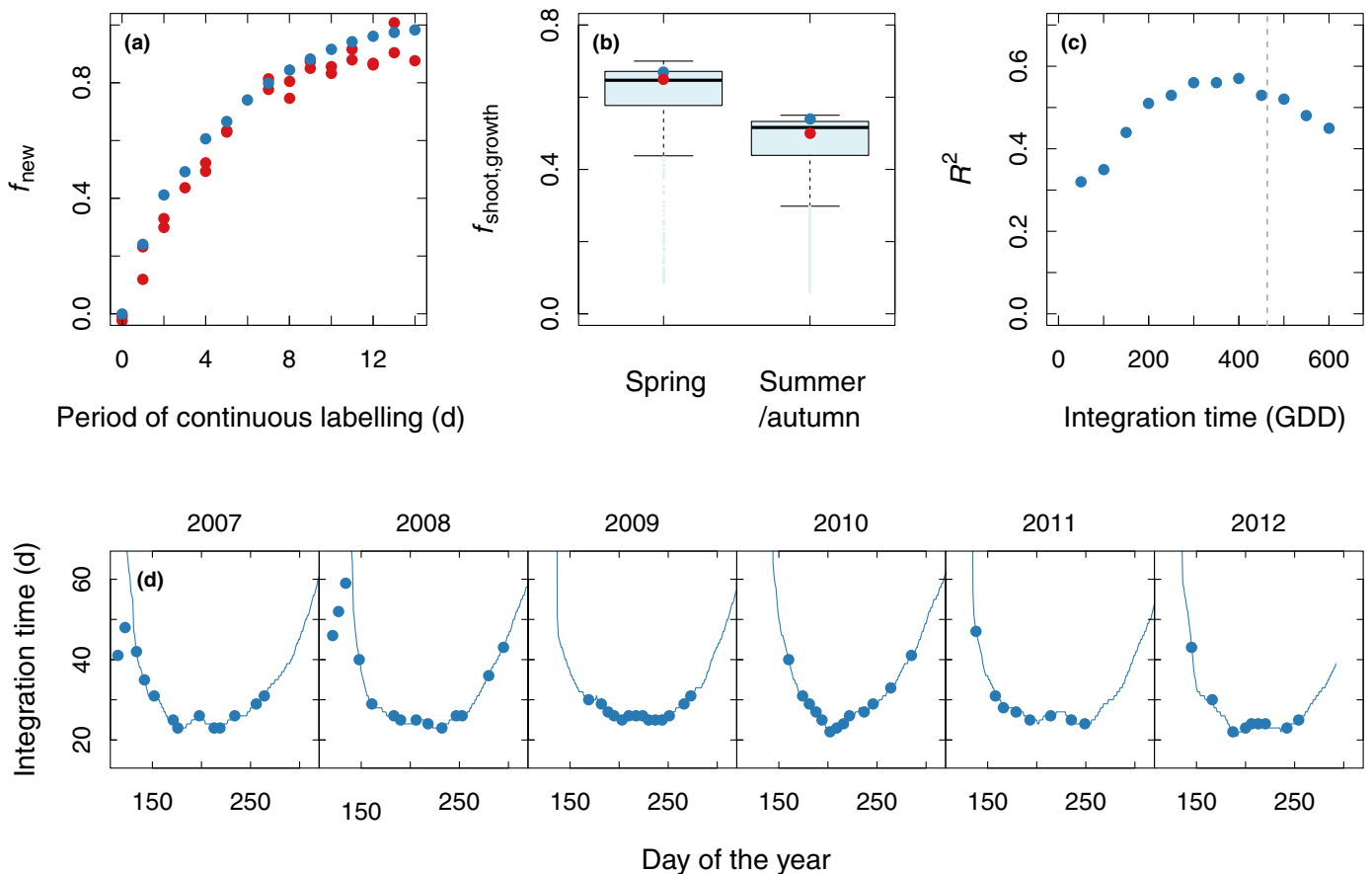


Fig. 4 (a) Fraction of labelled carbon (f_{new}) in total autotrophic respiration as obtained from a ^{13}C labelling kinetics study at the same experimental site in May 2007 (red points; Gamnitzer *et al.*, 2009), and dynamics of f_{new} in the metabolic pool (W_{pool}) induced by a step-change of $\delta^{13}\text{C}_{\text{CO}_2}$ in the MuSICA input data (blue points). (b) Boxplots showing the fraction of carbon allocated to shoot growth ($f_{shoot,growth}$) as predicted by the allocation-and-growth model for spring (mid-March to mid-June) and summer/autumn (mid-June to end-October) periods of the study years 2007–2012. Lower whiskers represent the smallest $f_{shoot,growth}$ values that are less than 1.5 times the interquartile range below the 25th percentile, and upper whiskers represent the maximum $f_{shoot,growth}$ for each period. Red points indicate $f_{shoot,growth}$ as estimated by ^{13}C -labelling for two 2-wk periods in May and September 2007 (Schleip, 2013), and blue points denote the model predictions for the same 2-wk periods. (c) R^2 values for the comparison between predicted and observed $\delta^{18}\text{O}_{\text{cellulose}}$. Model predictions were obtained using integration times between 50 and 600 growing-degree-days (GDD). The vertical dashed line indicates the average leaf lifespan observed by Schleip *et al.* (2013) for four co-dominant species of the same pasture investigated in this study. (d) Integration times (Δt) calculated from soil temperature and assuming a constant thermal age of 400 GDD with a base temperature of 4°C (see Eqn S8 in Supporting Information Methods S2). The blue points mark the days on which sampling occurred. It was assumed that leaf growth did not start before 15 March.

of $\Delta^{18}\text{O}_{\text{cellulose}}$ resembled only loosely that of $\delta^{18}\text{O}_{\text{cellulose}}$ ($R^2 = 0.18$ for the entire data set).

$\Delta^{18}\text{O}_{\text{cellulose}}$ showed statistically significant relationships with most meteorological variables averaged over the respective integration time (Table 2; Fig. 6). The correlation of $\Delta^{18}\text{O}_{\text{cellulose}}$ with midday RH ($r = -0.69$) was stronger than with daily mean air temperature ($r = -0.43$) and midday air temperature ($r = -0.37$). $\Delta^{18}\text{O}_{\text{cellulose}}$ was only weakly related to PAW in the rooting zone ($r = -0.24$; $P = 0.05$) and there were no statistically significant relationships with vapour pressure deficit (VPD) or annual precipitation (both $P > 0.05$). Correlation analysis also indicated connections between $\Delta^{18}\text{O}_{\text{cellulose}}$ and cumulative short-wave radiation ($r = 0.81$) and wind speed ($r = 0.56$). Yet, a sensitivity analysis in which the radiation input was halved or doubled demonstrated that cumulative short-wave radiation itself had only a very small effect on $\Delta^{18}\text{O}_{\text{cellulose}}$ (Fig. S1), indicating

that the strong correlation with $\Delta^{18}\text{O}_{\text{cellulose}}$ was indirect and arose primarily from the relationship of short-wave radiation with midday RH ($r = -0.63$) and temperature ($r = 0.57$) (Table S1). Sensitivity analysis also indicated that wind speed itself had a negligible effect on $\Delta^{18}\text{O}_{\text{cellulose}}$ (Fig. S1).

$\delta^{18}\text{O}_{\text{cellulose}}$ also had a clear relationship with RH ($r = -0.45$). Unlike $\Delta^{18}\text{O}_{\text{cellulose}}$, $\delta^{18}\text{O}_{\text{cellulose}}$ was related to precipitation amount ($r = -0.40$) and PAW ($r = -0.58$), with the latter negatively related to $\delta^{18}\text{O}_{\text{rain}}$ (Fig. S2a). Other relationships between $\delta^{18}\text{O}_{\text{cellulose}}$ and meteorological variables were weak (short-wave downward radiation) or nonsignificant (daily mean or midday air temperature, VPD, windspeed) (Table 2; Fig. 6).

Prediction of $\delta^{18}\text{O}_{\text{cellulose}}$ and $\Delta^{18}\text{O}_{\text{cellulose}}$

The standard model, with RH-sensitive $p_{ex}p_x$ and temperature-sensitive ϵ_{bio} , was able to reproduce with great accuracy the

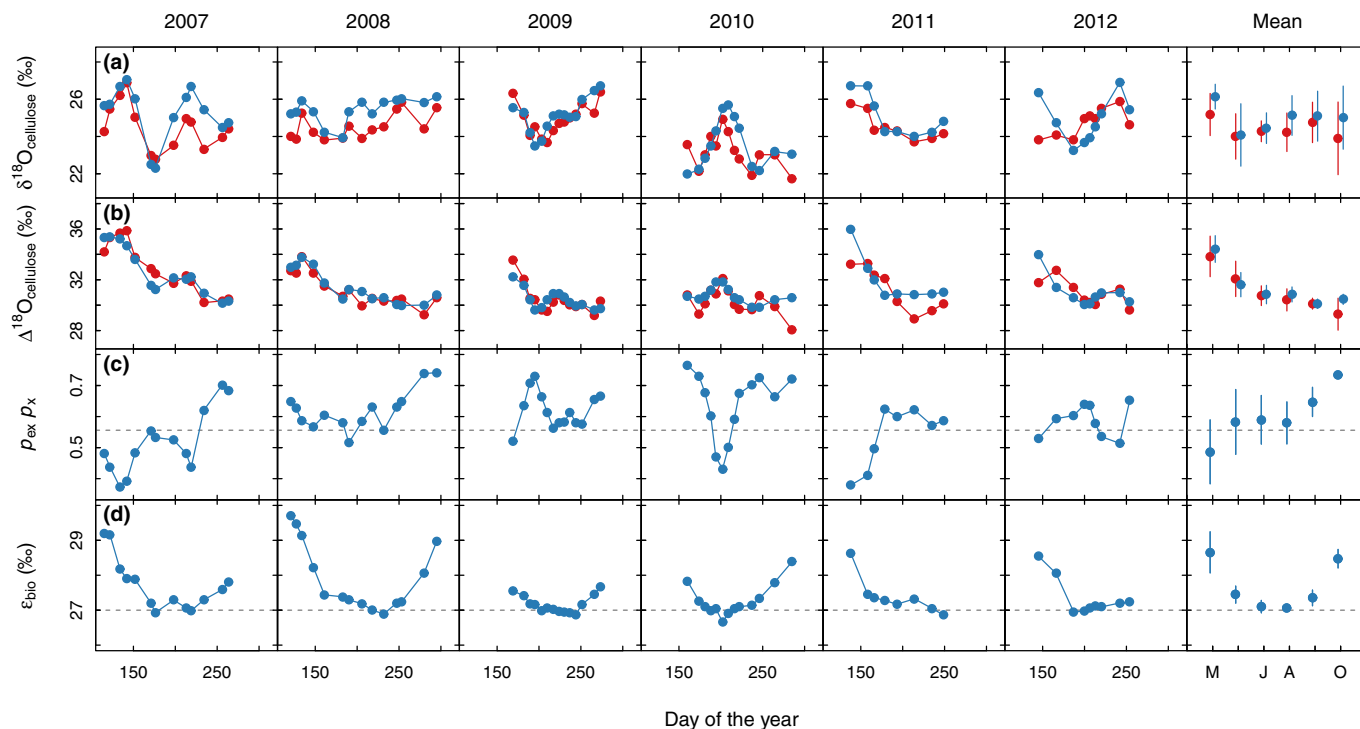


Fig. 5 Time course (a) of the oxygen isotope composition of leaf cellulose ($\delta^{18}\text{O}_{\text{cellulose}}$) and (b) of the isotopic enrichment of cellulose relative to source water ($\Delta^{18}\text{O}_{\text{cellulose}}$). Red dots, observed data; blue dots, model predictions obtained with the 'standard parameterization' with temperature-dependent ϵ_{bio} and RH-dependent $p_{\text{ex}}p_x$. Observed $\Delta^{18}\text{O}_{\text{cellulose}}$ was calculated from the $\delta^{18}\text{O}_{\text{cellulose}}$ of the sample and average observed $\delta^{18}\text{O}_{\text{source}}$ during 400 GDD before the sampling date (see Eqn S10 in Supporting Information Methods S2). (c) Time course of $p_{\text{ex}}p_x$ as estimated from midday relative humidity and averaged over the integration time (400 GDD). The horizontal dashed line indicates the value for $p_{\text{ex}}p_x$ used in the constant- $p_{\text{ex}}p_x$ simulations ($p_{\text{ex}}p_x = 0.556$). (d) Calculated average ϵ_{bio} for the total substrate used in cellulose synthesis of a given leaf sample throughout the 400 GDD integration time. The horizontal dashed line shows $\epsilon_{\text{bio}} = 27\text{‰}$. Average (2007–2012) monthly values of $\Delta^{18}\text{O}_{\text{cellulose}}$, $\delta^{18}\text{O}_{\text{cellulose}}$, $p_{\text{ex}}p_x$ and ϵ_{bio} are displayed on the right-hand side, with error bars denoting the standard deviations. Linear regression analysis indicated a significant trend for monthly mean $\Delta^{18}\text{O}_{\text{cellulose}}$ (observed $\Delta^{18}\text{O}_{\text{cellulose}} = 37.28 - 0.83 \text{ month}$; $R^2 = 0.90$; $P < 0.01$; predicted $\Delta^{18}\text{O}_{\text{cellulose}} = 36.59 - 0.69 \text{ month}$; $R^2 = 0.68$; $P < 0.05$) and monthly mean $p_{\text{ex}}p_x$ ($p_{\text{ex}}p_x = 0.30 + 0.04 \text{ month}$; $R^2 = 0.85$; $P < 0.01$).

observed seasonal dynamics of $\delta^{18}\text{O}_{\text{cellulose}}$ ($R^2 = 0.57$) and $\Delta^{18}\text{O}_{\text{cellulose}}$ ($R^2 = 0.74$) over the entire 6-yr-long study period (Figs 5, 7d). The model error and bias were small (Table 3), as the model was also able to capture the short-term variations. By contrast, predictions of $\Delta^{18}\text{O}_{\text{cellulose}}$ made with constant $p_{\text{ex}}p_x$ and/or constant ϵ_{bio} degraded significantly the goodness-of-fit with observed $\Delta^{18}\text{O}_{\text{cellulose}}$ (Fig. 7a–c).

Variation of midday RH at the study site, averaged over the integration time, was significant (47–73%) and implied a large range of modelled $p_{\text{ex}}p_x$ (0.37–0.77; average: 0.59), with a generally increasing trend during the growing season (Fig. 5c). Meanwhile, daily mean air temperature varied considerably at the scale of integration times (between 7 and 22°C), leading to pronounced variation in ϵ_{bio} (from 26 to 30‰; Fig. 5d). ϵ_{bio} generally decreased from spring to summer and increased towards late autumn. The ability of the model to reproduce the observed relationships between $\Delta^{18}\text{O}_{\text{cellulose}}$ (or $\delta^{18}\text{O}_{\text{cellulose}}$) and meteorological variables or PAW also depended on the inclusion of an RH-sensitive $p_{\text{ex}}p_x$ and a temperature-sensitive ϵ_{bio} (Table 2). In particular, the model was unable to reproduce the observed relationship between $\Delta^{18}\text{O}_{\text{cellulose}}$ and air temperature when a constant

ϵ_{bio} of 27‰ was used instead of a temperature-dependent one (Fig. S3d–f).

Relationship between canopy conductance and $\Delta^{18}\text{O}_{\text{cellulose}}$ or $\delta^{18}\text{O}_{\text{cellulose}}$

Observed $\Delta^{18}\text{O}_{\text{cellulose}}$ was negatively related to midday canopy conductance predicted by the MuSICA model ($R^2 = 0.26$; $P < 0.001$; Table 2; Fig. 8), with a 100 $\text{mmol m}^{-2} \text{ s}^{-1}$ increase in g_{canopy} connected to a 1.4‰ decrease of $\Delta^{18}\text{O}_{\text{cellulose}}$. Again, the relationship between midday canopy conductance and observed or predicted $\Delta^{18}\text{O}_{\text{cellulose}}$ was the same if the prediction was based on RH-sensitive $p_{\text{ex}}p_x$ and temperature-sensitive ϵ_{bio} , but not if constants for $p_{\text{ex}}p_x$ or ϵ_{bio} were used.

The relationship between observed $\delta^{18}\text{O}_{\text{cellulose}}$ and modelled midday canopy conductance was also negative ($P < 0.05$), although the slope and R^2 for that relationship were much smaller than those for $\Delta^{18}\text{O}_{\text{cellulose}}$. The relationship between predicted $\delta^{18}\text{O}_{\text{cellulose}}$ and modelled canopy conductance was similar to the observations when predictions were based on RH-sensitive $p_{\text{ex}}p_x$ and temperature-sensitive ϵ_{bio} , and became

Table 2 Regression equations for the relationships of observed and predicted $\Delta^{18}\text{O}_{\text{cellulose}}$ and $\delta^{18}\text{O}_{\text{cellulose}}$ with meteorological variables at Grünschwaige pasture paddock no. 8.

	$\Delta^{18}\text{O}_{\text{cellulose}}$		$\delta^{18}\text{O}_{\text{cellulose}}$	
	Observed	Predicted	Observed	Predicted
RH	$\Delta^{18}\text{O} = 42.60 - 0.19\text{RH};$ $R^2 = 0.48; P < 0.001$	$\Delta^{18}\text{O} = 42.42 - 0.18\text{RH};$ $R^2 = 0.51; P < 0.001$	$\delta^{18}\text{O} = 29.31 - 0.08\text{RH};$ $R^2 = 0.21; P < 0.001$	$\delta^{18}\text{O} = 32.22 - 0.12\text{RH};$ $R^2 = 0.31; P < 0.001$
Daily mean T_{air}	$\Delta^{18}\text{O} = 34.65 - 0.21T_{\text{air}};$ $R^2 = 0.19; P < 0.001$	$\Delta^{18}\text{O} = 35.65 - 0.26T_{\text{air}};$ $R^2 = 0.32; P < 0.001$	ns	ns
Midday T_{air}	$\Delta^{18}\text{O} = 34.59 - 0.18T_{\text{air}};$ $R^2 = 0.14; P < 0.01$	$\Delta^{18}\text{O} = 35.66 - 0.22T_{\text{air}};$ $R^2 = 0.25; P < 0.001$	ns	ns
VPD	ns	ns	ns	$\delta^{18}\text{O} = 23.69 + 1.19\text{VPD};$ $R^2 = 0.05; P = 0.049$
PAW	$\Delta^{18}\text{O} = 32.04 - 0.03\text{PAW};$ $R^2 = 0.06; P = 0.0476$	ns	$\delta^{18}\text{O} = 25.80 - 0.04\text{PAW};$ $R^2 = 0.33; P < 0.001$	$\delta^{18}\text{O} = 26.58 - 0.05\text{PAW};$ $R^2 = 0.32; P < 0.001$
Precip	ns	ns	$\delta^{18}\text{O} = 25.26 - 0.01\text{Rain};$ $R^2 = 0.16; P < 0.001$	$\delta^{18}\text{O} = 25.90 - 0.01\text{Rain};$ $R^2 = 0.14; P < 0.01$
Short-wave radiation	$\Delta^{18}\text{O} = 25.91 + 0.01R_{\text{s}\downarrow};$ $R^2 = 0.65; P < 0.001$	$\Delta^{18}\text{O} = 25.82 + 0.01R_{\text{s}\downarrow};$ $R^2 = 0.83; P < 0.001$	$\delta^{18}\text{O} = 23.38 + 0.002R_{\text{s}\downarrow};$ $R^2 = 0.06; P = 0.046$	$\delta^{18}\text{O} = 23.42 + 0.003R_{\text{s}\downarrow};$ $R^2 = 0.08; P = 0.015$
Wind speed	$\Delta^{18}\text{O} = 26.41 + 1.34u;$ $R^2 = 0.32; P < 0.001$	$\Delta^{18}\text{O} = 26.73 + 1.30u;$ $R^2 = 0.34; P < 0.001$	ns	ns

Relative humidity (RH), midday air temperature (Midday T_{air}), vapour pressure deficit (VPD), plant-available water (PAW) and wind speed (u) all represent midday (± 3 h around noon) values averaged over the integration time Δt (400 GDD). Daily mean T_{air} represents daily average air temperature over Δt , and precipitation amount (Precip) and short-wave radiation ($R_{\text{s}\downarrow}$) represent the precipitation sum and the total sum of incoming short-wave radiation within Δt . ns, not significant ($P > 0.05$).

insignificant when predictions used constant values for ϵ_{bio} , or $p_{\text{ex}p_x}$ and ϵ_{bio} .

Sensitivity to model parameters

Model predictions of $\delta^{18}\text{O}_{\text{cellulose}}$ or $\Delta^{18}\text{O}_{\text{cellulose}}$ were relatively insensitive to alterations of the parameters of the allocation-and-growth model (Table 1; Fig. S1), except for integration time (Fig. 4c). That is, both the mean sensitivity (i.e. the mean difference between the sensitivity run and standard run for predictions of $\delta^{18}\text{O}_{\text{cellulose}}$ (or $\Delta^{18}\text{O}_{\text{cellulose}}$)) as well as the standard deviation of the sensitivity was smaller than 0.2‰ for each parameter value (Fig. S1).

In the MuSICA model, a 2.5-fold increase of m_{gs} (see Table 1) – the slope of the Ball–Woodrow–Berry stomatal conductance model (Ball *et al.*, 1987) – caused an average reduction of 0.84‰ of the predicted $\delta^{18}\text{O}_{\text{cellulose}}$ and $\Delta^{18}\text{O}_{\text{cellulose}}$. For a particular situation (time), the size of that effect depended on the conditions prevailing during the respective integration time. This conditionality was reflected in the relatively high standard deviations between individual sensitivity and standard model runs for m_{gs} (Fig. S1). Conversely, a reduction of m_{gs} by one-third caused an average increase of 0.3‰, with the increase again dependent on prevailing conditions, as above. On the other hand, increasing V_{cmax} and J_{max} by 2.2-fold or reducing it by two-thirds had only small effects on the prediction of $\delta^{18}\text{O}_{\text{cellulose}}$ and $\Delta^{18}\text{O}_{\text{cellulose}}$ (mean sensitivity ≤ 0.32 ‰).

In general, predicted $\Delta^{18}\text{O}_{\text{cellulose}}$ decreased (increased) with increasing (decreasing) temperature in the sensitivity analysis (Fig. S4). If ϵ_{bio} was allowed to vary with temperature (corresponding to the default parameterization), a 1°C increase

(decrease) in temperature caused a 0.28‰ decrease (increase) in the predicted $\Delta^{18}\text{O}_{\text{cellulose}}$. Conversely, if ϵ_{bio} was set to be constant (at 27‰), the resulting temperature-sensitivity of predicted $\Delta^{18}\text{O}_{\text{cellulose}}$ was only -0.11 ‰ °C⁻¹.

Discussion

Estimates of isotopic signal integration time in cellulose agree with leaf lifespan and residence time of nonstructural carbon

This work presents a new allocation-and-growth model that generates realistic estimates for the turnover of the metabolic pool used to supply autotrophic respiration, the allocation of assimilates to shoot and root growth, and the integration (or residence time) of cellulose in growing leaf material in a drought-prone, temperate grassland ecosystem. When coupled to a recently published version of an ¹⁸O-enabled soil–vegetation–atmosphere transfer model (MuSICA) parameterized for a grassland (Hirl *et al.*, 2019), this allocation-and-growth model provided a faithful prediction of the fortnightly, seasonal and multi-annual variation of the ¹⁸O composition of cellulose in mixed-species leaf samples from this pasture ecosystem. The coupled model also enabled an explicit evaluation of the current theory of ¹⁸O-enrichment of cellulose ($\Delta^{18}\text{O}_{\text{cellulose}}$), namely the factors that determine the relationship between $\delta^{18}\text{O}_{\text{cellulose}}$ and $\delta^{18}\text{O}_{\text{source}}$ on the one hand and those of $\delta^{18}\text{O}_{\text{leaf}}$ on the other. We found compelling evidence that: ϵ_{bio} , the average biochemical fractionation between the organic substrate used for cellulose synthesis and water in the field, is temperature-dependent, in close agreement with studies of submerged aquatic plants as shown by

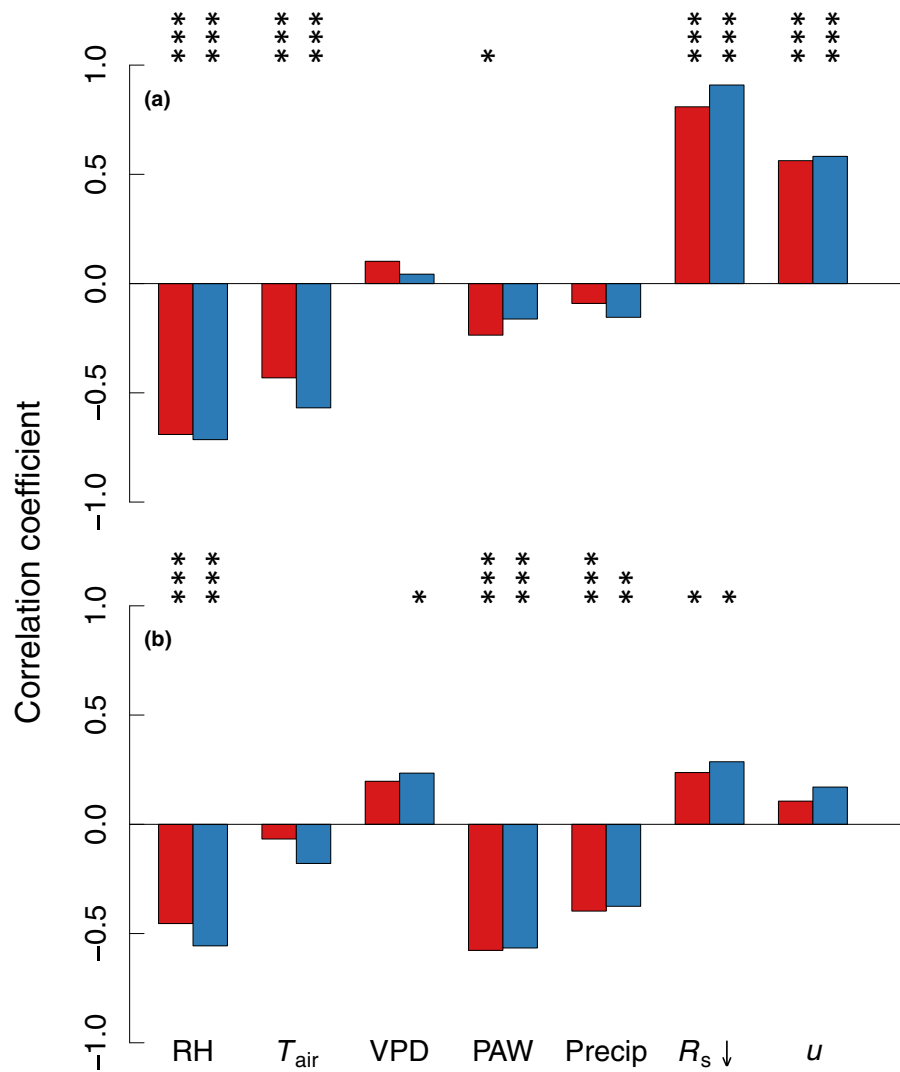


Fig. 6 Correlation coefficients for the relationships between (a) $\Delta^{18}\text{O}_{\text{cellulose}}$ and meteorological variables and (b) $\delta^{18}\text{O}_{\text{cellulose}}$ and meteorological variables: relative humidity (RH), air temperature (T_{air}), vapour pressure deficit of the air (VPD), plant-available water (PAW), precipitation amount (Precip), incoming (downward) short-wave radiation ($R_s \downarrow$) and wind speed (u). Red bars, observed data; blue bars, predicted data. RH, VPD and u represent midday (± 3 h around noon) values averaged over the integration time Δt (400 GDD); T_{air} represents daily mean values averaged over Δt ; and $R_s \downarrow$ and Precip represent the total sums of incoming short-wave radiation and the total precipitation within Δt . All predictions were made with the model in 'standard parameterization', including temperature-sensitive ϵ_{bio} and relative humidity-sensitive $p_{\text{ex}p_x}$. Asterisks indicate the significance levels: ***, $P < 0.001$; **, $P < 0.01$; *, $P < 0.05$.

Sternberg & Ellsworth (2011); and $p_{\text{ex}p_x}$, the proportion of oxygen in cellulose derived from source water, responded to RH in accordance with the findings of Lehmann *et al.* (2017) and our own investigations (unpublished data) with *L. perenne* in controlled environments.

To predict $\delta^{18}\text{O}_{\text{cellulose}}$ accurately, the integration time used in the model calculations was particularly important. Model-data comparison of $\delta^{18}\text{O}_{\text{cellulose}}$ indicated a best match with 400 GDD. This was 14% shorter than the average observed leaf lifespan (LLS; 463 ± 56 GDD) of the main species (*L. perenne*, *P. pratensis*, *T. officinale* and *T. repens*) at the same site (Schleip *et al.*, 2013). A possible explanation is that Schleip *et al.* considered that LLS ended when a senescing leaf had 25% chlorotic tissue while leaf sampling for the present investigation comprised

only fully green leaf blades and excluded any chlorotic leaf blades. Therefore, the collected leaves were probably not older than *c.* 320–450 GDD (compare with fig. 2 in Schleip *et al.*, 2013), in close agreement with the observed best match for an integration time of *c.* 400 GDD (Fig. 4c). This value also agrees well with the mean residence time of structural carbon in above-ground biomass of the codominant species at the same site observed by Ostler *et al.* (2016).

First field-based evidence for a strong temperature effect on ϵ_{bio} , in agreement with laboratory studies

Over the integration time, air temperature ranged from 7 to 22°C and midday RH from 47 to 73%. Importantly, however,

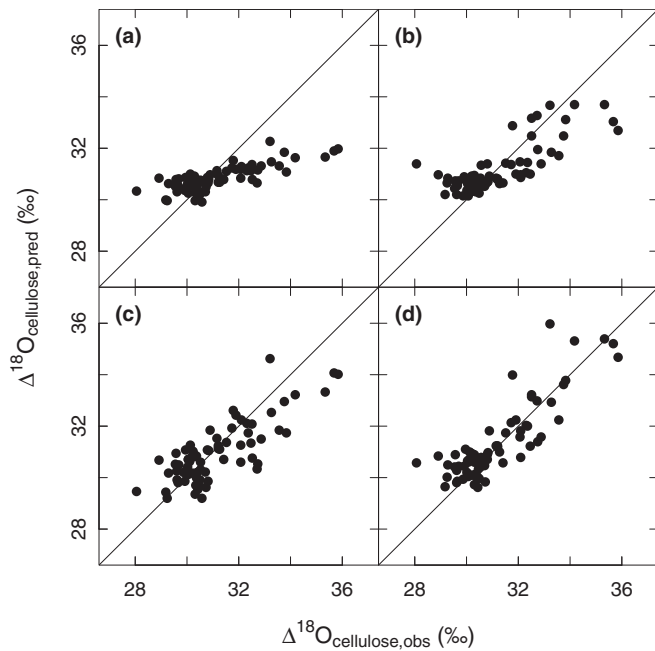


Fig. 7 Scatter plots showing the relationship between predicted and observed ^{18}O -enrichment of cellulose relative to source water ($\Delta^{18}\text{O}_{\text{cellulose}}$) for predictions based on (a) $\epsilon_{\text{bio}} = 27\text{‰}$ and $p_{\text{exp}P_x} = 0.556$, (b) temperature-dependent ϵ_{bio} and $p_{\text{exp}P_x} = 0.556$, (c) $\epsilon_{\text{bio}} = 27\text{‰}$ and RH-dependent $p_{\text{exp}P_x}$, and (d) temperature-dependent ϵ_{bio} and RH-dependent $p_{\text{exp}P_x}$ (i.e. the ‘standard simulation’). Solid lines indicate the 1 : 1 line.

Table 3 R^2 , mean bias error (MBE) and mean absolute error (MAE) for the comparison between predicted and observed $\delta^{18}\text{O}_{\text{cellulose}}$ or $\Delta^{18}\text{O}_{\text{cellulose}}$ at Grünschwaipe pasture paddock no. 8.

	R^2	MBE	MAE
Standard simulation			
$\delta^{18}\text{O}_{\text{cellulose}}$	0.57	0.5	0.8
$\Delta^{18}\text{O}_{\text{cellulose}}$	0.74	0.2	0.6
Const. ϵ_{bio} ; const. $p_{\text{exp}P_x}$:			
$\delta^{18}\text{O}_{\text{cellulose}}$	0.26	0	0.8
$\Delta^{18}\text{O}_{\text{cellulose}}$	0.62	-0.3	0.9
Var. ϵ_{bio} ; const. $p_{\text{exp}P_x}$:			
$\delta^{18}\text{O}_{\text{cellulose}}$	0.40	0	0.8
$\Delta^{18}\text{O}_{\text{cellulose}}$	0.63	0	0.8
Const. ϵ_{bio} ; var. $p_{\text{exp}P_x}$:			
$\delta^{18}\text{O}_{\text{cellulose}}$	0.49	0.2	0.8
$\Delta^{18}\text{O}_{\text{cellulose}}$	0.64	-0.2	0.8

Predictions were made with the standard parameterization of the model (T_{air} -dependent ϵ_{bio} ; RH-dependent $p_{\text{exp}P_x}$), and with constant $\epsilon_{\text{bio}} = 27\text{‰}$ and constant $p_{\text{exp}P_x} = 0.556$, or constant $\epsilon_{\text{bio}} = 27\text{‰}$ and RH-dependent $p_{\text{exp}P_x}$. Constant and variable (i.e. T_{air} -dependent ϵ_{bio} or RH-dependent $p_{\text{exp}P_x}$) parameters are coded as ‘Const.’ and ‘Var.’ in the table entries above. MBE and MAE values are given in per mil (‰). The MAE between the $\delta^{18}\text{O}$ values of the replicate samples collected on the different dates was 0.4‰.

variations of RH and temperature were not significantly correlated at the integration time-scale ($P = 0.50$), meaning that RH and air temperature varied largely independently from each other. This factor aided/enabled the identification and distinction of the RH effect on $p_{\text{exp}P_x}$ and of the temperature effect on ϵ_{bio} .

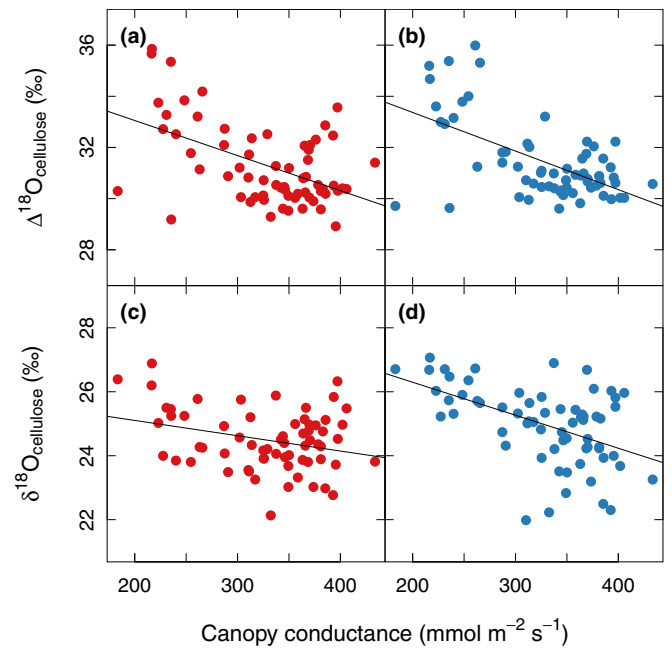


Fig. 8 Relationships between (a and b) $\Delta^{18}\text{O}_{\text{cellulose}}$ and canopy conductance, and (c and d) $\delta^{18}\text{O}_{\text{cellulose}}$ and canopy conductance. (a, c) Observed relationships, (b, d) predicted relationships obtained with the model in standard parameterization with temperature-dependent ϵ_{bio} and RH-dependent $p_{\text{exp}P_x}$. Canopy conductance was modelled for midday (± 3 h around noon) conditions averaged over the integration time Δt and with the model in standard parameterization (Hirl *et al.*, 2019). Solid lines represent the linear regression lines: (a) $\Delta^{18}\text{O} = 35.79 - 0.014g_s$; $R^2 = 0.26$; $P < 0.001$; (b) $\Delta^{18}\text{O} = 36.38 - 0.015g_s$; $R^2 = 0.33$; $P < 0.001$; (c) $\delta^{18}\text{O} = 26.06 - 0.005g_s$; $R^2 = 0.09$; $P = 0.017$; (d) $\delta^{18}\text{O} = 28.36 - 0.01g_s$; $R^2 = 0.25$; $P < 0.001$.

Notably, daily mean temperatures over the integration time covered most of the temperature-sensitive range of ϵ_{bio} (Sternberg & Ellsworth, 2011), explaining why the inclusion of a temperature-dependent ϵ_{bio} was so critical for simulating $\Delta^{18}\text{O}_{\text{cellulose}}$. Unfortunately, it is presently unknown how temperature influences the relevant biochemical mechanisms and their associated isotope effects that combine to yield the ‘average biochemical fractionation between substrate for cellulose synthesis and water’ ϵ_{bio} . In that regard, however, it is interesting and encouraging that the temperature-dependence of ϵ_{bio} observed here matched closely the patterns observed by Sternberg & Ellsworth (2011) in aquatic and heterotrophic systems. To the best of our knowledge, convincing general, field-based evidence supporting the requirement of a temperature-sensitive ϵ_{bio} has not been published so far. Still, a possible temperature-sensitivity of ϵ_{bio} has been discussed in modelling studies on tree-ring $\delta^{18}\text{O}_{\text{cellulose}}$ by Keel *et al.* (2016) and Lavergne *et al.* (2017) on tree species from different functional groups growing across a range of temperate to cold environments. Partial evidence in favour of a temperature-sensitive ϵ_{bio} was presented by both groups, although overall evidence was inconclusive because of uncertainties in either the models or the climate and site data. Strong evidence for a temperature-sensitive ϵ_{bio} is reinforced in our comprehensive model parameterization and validation study against an extensive field dataset. In particular, the leaf water modelling, partitioning of source ($\delta^{18}\text{O}_{\text{source}}$)

and enrichment effects ($\Delta^{18}\text{O}_{\text{leaf}}$) on leaf water isotope composition ($\delta^{18}\text{O}_{\text{leaf}}$) (Hirl *et al.*, 2019) permitted a very robust modelling of $\Delta^{18}\text{O}_{\text{cellulose}}$ that could be contrasted with observations of $\Delta^{18}\text{O}_{\text{cellulose}}$, across a multiyear dataset using the same set of model parameters.

Sensitivity analyses of temperature effects on predictions of $\Delta^{18}\text{O}_{\text{cellulose}}$ demonstrated that *c.* 60% of the temperature effect in $\Delta^{18}\text{O}_{\text{cellulose}}$ was related to ϵ_{bio} , with the remaining 40% connected to all other temperature-dependent processes influencing $\Delta^{18}\text{O}_{\text{cellulose}}$. Interestingly, the temperature sensitivity of $\Delta^{18}\text{O}_{\text{cellulose}}$ ($-0.28\text{‰ } ^\circ\text{C}^{-1}$) was similar in magnitude but opposite in sign to the temperature sensitivity of $\delta^{18}\text{O}_{\text{rain}}$ ($+0.36\text{‰ } ^\circ\text{C}^{-1}$; Fig. S2b). This caused a lack of correlation between $\delta^{18}\text{O}_{\text{cellulose}}$ and temperature, and highlights the need (and benefit) of studying both $\Delta^{18}\text{O}_{\text{cellulose}}$ and $\delta^{18}\text{O}_{\text{cellulose}}$. Previous studies found a significant correlation between $\delta^{18}\text{O}_{\text{cellulose}}$ (mainly from tree rings) and temperature. These studies used different temporal (decadal or century-scale changes in contrast to the seasonal patterns studied here), spatial (latitudinal or altitudinal, as compared to the stationary observations in the present study) or aridity gradients, and may have also differed in the temperature sensitivity of $\Delta^{18}\text{O}_{\text{cellulose}}$ relative to that of $\delta^{18}\text{O}_{\text{rain}}$ (e.g. Anderson *et al.*, 1998; Saurer *et al.*, 2002; Kress *et al.*, 2010; Song *et al.*, 2011).

Evidence for an increase of $p_{\text{ex}}p_x$ with air humidity, possibly linked to leaf water ^{18}O -enrichment along leaf blades

Model-data comparison also strongly supported the inclusion of an RH-dependent $p_{\text{ex}}p_x$ in the computation of $\Delta^{18}\text{O}_{\text{cellulose}}$. This RH dependency of $p_{\text{ex}}p_x$ was derived from the relationship between RH and the model-data residuals when $\Delta^{18}\text{O}_{\text{cellulose}}$ was predicted with a constant $p_{\text{ex}}p_x$ of 0.556, combined with Eqns S7 and S9 (see Methods S2 and S3). A similar agreement between predicted and observed data was obtained when using the RH-sensitivity of $p_{\text{ex}}p_x$ observed by Lehmann *et al.* (2017) in a controlled environment study with *L. perenne* and *D. glomerata*, two of the codominant species present in our system. The RH dependency of $p_{\text{ex}}p_x$ required to link $\Delta^{18}\text{O}_{\text{cellulose}}$ and $\Delta^{18}\text{O}_{\text{leaf}}$ has been discussed previously for a range of C_3 and C_4 grasses (Liu *et al.*, 2016). Failure to predict $\Delta^{18}\text{O}_{\text{cellulose}}$ with a constant (i.e. RH-insensitive) $p_{\text{ex}}p_x$ was not related to erroneous MuSICA predictions of $\Delta^{18}\text{O}_{\text{leaf}}$, as these exhibited a virtually identical RH-response to observed $\Delta^{18}\text{O}_{\text{leaf}}$ (Hirl *et al.*, 2019). Predictions of $\Delta^{18}\text{O}_{\text{assim}}$ by MuSICA were based on bulk leaf water $\Delta^{18}\text{O}_{\text{leaf}}$ and the common assumption that new assimilates are in isotopic equilibrium with $\Delta^{18}\text{O}_{\text{leaf}}$ ($\Delta^{18}\text{O}_{\text{assim}} = \Delta^{18}\text{O}_{\text{leaf}} + \epsilon_{\text{bio}}$; Barbour, 2007). Lehmann *et al.* (2017) showed that this assumption may not always hold in grasses where RH was affecting the $\delta^{18}\text{O}$ of sucrose ($\delta^{18}\text{O}_{\text{sucrose}}$) more strongly than $\delta^{18}\text{O}_{\text{leaf}}$. These results support the view that $\Delta^{18}\text{O}_{\text{sucrose}}$ is not always equal to $\Delta^{18}\text{O}_{\text{leaf}} + \epsilon_{\text{bio}}$ in grasses, and that RH affects the divergence between $\Delta^{18}\text{O}_{\text{leaf}}$ and the $\Delta^{18}\text{O}$ of the water in which assimilation and sucrose synthesis takes place ($\Delta^{18}\text{O}_{\text{suc-water}}$). This divergence between $\Delta^{18}\text{O}_{\text{leaf}}$ and $\Delta^{18}\text{O}_{\text{suc-water}}$ may be related to the gradient of ^{18}O enrichment along leaf blades observed by Helliker & Ehleringer (2000, 2002a) and Gan *et al.* (2003), which is

particularly steep at low RH. Uncertainties on $\Delta^{18}\text{O}_{\text{suc-water}}$ affect the calculation of $p_{\text{ex}}p_x$. p_x is commonly calculated from a two-end-member mixing model, the end-members being the $\Delta^{18}\text{O}$ of water at the site of cellulose synthesis ($\Delta^{18}\text{O}_{\text{cel-water}}$) and $\Delta^{18}\text{O}_{\text{suc-water}}$, with the latter approximated as $\Delta^{18}\text{O}_{\text{leaf}}$: $p_x = 1 - \Delta^{18}\text{O}_{\text{cel-water}}/\Delta^{18}\text{O}_{\text{suc-water}}$. A deviation between $\Delta^{18}\text{O}_{\text{suc-water}}$ and $\Delta^{18}\text{O}_{\text{leaf}}$ affects the calculation of p_x . However, for grasses, this error must be small, as the water in the leaf growth and differentiation zone of grasses is close to source water ($\Delta^{18}\text{O}_{\text{cel-water}}$ of *c.* 0) so that p_x is *c.* 1 (Liu *et al.*, 2017a). Accordingly, the divergence between $\Delta^{18}\text{O}_{\text{suc-water}}$ and $\Delta^{18}\text{O}_{\text{leaf}}$ noted by Lehmann *et al.* (2017) mostly affects the estimate of p_{ex} .

Other factors that have been related to variations of p_{ex} have included ^{18}O -exchange during phloem transport from the leaves to the growing tissue (Gessler *et al.*, 2007; but see Gessler *et al.*, 2013) and futile cycling of the growth substrate within the growing tissue (Barbour, 2007), potentially linked to cellular growth rate or other cellular anatomical features, such as the lumen area of cambial cells (Szejner *et al.*, 2020). The rate of futile cycling has been related to the turnover of the water-soluble carbohydrate pool in *Ricinus communis* (Song *et al.*, 2014). However, we could not detect a significant relationship between the modelled mean residence time of substrate in the metabolic pool (τ_{pool}) and p_{ex} , estimated from $p_{\text{ex}}p_x$ with $p_x = 1$ (Fig. S5), although statistical noise may have been a factor. Also, modelled integration time (in days) – which is a function of leaf appearance, growth and senescence rates that are all closely coordinated in grasses (Lemaire *et al.*, 2000; Schleip *et al.*, 2013) – did not correlate with estimates of p_{ex} . Lastly, in a recent study, we did not observe an effect of RH on the hydraulic conductance of *L. perenne* vegetative plants in controlled environments (Baca Cabrera *et al.*, 2020), providing no (physiological) indication of an effect of RH on xylem lumen area. Clearly, there is a great need for detailed biochemical investigations of the factors underlying the variation of p_{ex} .

Predictions of canopy conductance from ^{18}O -enrichment of cellulose required a temperature-dependent ϵ_{bio} and humidity-sensitive $p_{\text{ex}}p_x$

Finally, this work demonstrates a significant negative relationship between midday canopy conductance (g_{canopy}) and both $\Delta^{18}\text{O}_{\text{cellulose}}$ and $\delta^{18}\text{O}_{\text{cellulose}}$. Although used in multiple studies to interpret variation in $\Delta^{13}\text{C}$ and intrinsic water-use efficiency, experimental or empirical evidence for the relationship between $\Delta^{18}\text{O}_{\text{cellulose}}$ (or $\delta^{18}\text{O}_{\text{cellulose}}$) and stomatal or canopy conductance is relatively scarce (Barbour *et al.*, 2000; Grams *et al.*, 2007; Sullivan & Welker, 2007; Moreno-Gutiérrez *et al.*, 2012). In principle, the correlation between g_{canopy} and $\Delta^{18}\text{O}_{\text{cellulose}}$ could be caused by any environmental factor that affects stomatal opening and consequently alters leaf temperature, leaf-to-air vapour pressure difference, and thus $\Delta^{18}\text{O}_{\text{leaf}}$, $\Delta^{18}\text{O}_{\text{suc-water}}$, ϵ_{bio} and ultimately $\Delta^{18}\text{O}_{\text{cellulose}}$. Correlations between $\Delta^{18}\text{O}_{\text{cellulose}}$ and stomatal conductance observed in previous studies were evoked by treatment differences in air CO_2 and O_3 concentration and by interplant competition (Grams *et al.*, 2007), or by variation in soil temperature and soil water status (Sullivan & Welker, 2007).

In a previous study, we found a significant effect of both soil water content and RH on $\Delta^{18}\text{O}_{\text{leaf}}$, and a significant relationship between soil moisture and canopy conductance (Hirl *et al.*, 2019). Remarkably, however, we could not identify a drought-related increase of $\Delta^{18}\text{O}_{\text{cellulose}}$, which would indicate a drought-related decrease of stomatal conductance (Fig. S6). We believe that absence of a drought signal in $\Delta^{18}\text{O}_{\text{cellulose}}$ is caused by the low assimilation rate and deceleration (or complete cessation) of leaf growth under drought. By contrast, both $\Delta^{18}\text{O}_{\text{cellulose}}$ (Table 2; Fig. 6; Fig. S3a,c) and g_{canopy} ($R^2 = 0.13$; $P < 0.01$) were significantly related to RH. The RH-sensitivity of $\Delta^{18}\text{O}_{\text{cellulose}}$ was even higher than that of $\Delta^{18}\text{O}_{\text{leaf}}$ ($-0.15\text{‰}\ \text{‰}^{-1}$), due to the relationship between RH and $p_{\text{ex}}p_x$ (as already discussed). If $\Delta^{18}\text{O}_{\text{suc-water}}$ is more strongly related to evaporative conditions than $\Delta^{18}\text{O}_{\text{leaf}}$, the stomatal conductance signal in cellulose may in fact be more pronounced than previously expected solely from the climate-sensitivity of bulk leaf water. This lends further support to studies that aim to reconstruct stomatal conductance from $\delta^{18}\text{O}_{\text{cellulose}}$.

Conclusions and perspective

This study provides strong evidence for important climate-sensitive variation of the parameters $p_{\text{ex}}p_x$ and ϵ_{bio} of the Barbour–Farquhar model in a terrestrial ecosystem. Elucidation of those sensitivities demanded and relied on the use of a carefully parameterized, ^{18}O -enabled process-based soil–plant–atmosphere transfer model and the existence of a detailed multiseasonal observational data set of ^{18}O signals in all relevant ecosystem water pools and leaf cellulose. As a result, our work demonstrates at the ecosystem scale the validity of earlier conclusions that were drawn from model-type, experimental studies conducted in steady-state, controlled environments, but have not been generally considered in the relevant fields of terrestrial ecosystem sciences. Our results have important implications for the interpretation of seasonal, interannual and geographical variations of $\Delta^{18}\text{O}_{\text{cellulose}}$ and $\delta^{18}\text{O}_{\text{cellulose}}$ in terms of plant physiology and climate. Existing datasets, for example on tree-ring $\Delta^{18}\text{O}_{\text{cellulose}}$ or $\delta^{18}\text{O}_{\text{cellulose}}$ from boreal to subtropical ecosystems, should benefit from a re-evaluation that considers the varying nature of biochemical fractionation and isotopic exchange with source and leaf water. In addition, there is a great need for more targeted studies investigating the mechanisms underlying the large observed effect of temperature on ϵ_{bio} and the RH-dependent variation of $p_{\text{ex}}p_x$. Such knowledge will help us to better understand the physiological information that is imprinted in cellulose- ^{18}O signals from past and present environments.

Acknowledgements

We thank Erna Eschenbach†, Angela Ernst-Schwärzli, Anja Schmidt, Monika Michler, Hans Vogl, Richard Wenzel and Lenka Plavcová for technical assistance, and Iris Köhler for previous discussion. JZ was supported by the China Scholarship Council. We are grateful to Xin Song and two anonymous reviewers for

constructive comments. This work was supported by the Deutsche Forschungsgemeinschaft (DFG SCHN 557/9-1).

Author contributions

RTH, JO and HS designed the research. RTH, UO and HS designed the allocation-and-growth model. RTH analysed the data and performed the modelling with guidance by JO and UO. RS performed the isotope analysis. HS, UO and IS designed and UO and IS performed the tracer experiment. HS and RTH planned and RTH, JCBC and JZ performed the mesocosm experiment. RTH wrote the first draft. RTH, JO, UO, RS, JCBC, JZ, IS, LW and HS contributed to the discussion and the revision of the manuscript.

ORCID

Juan C. Baca Cabrera  <https://orcid.org/0000-0001-8159-3837>
 Jérôme Ogée  <https://orcid.org/0000-0002-3365-8584>
 Ulrike Ostler  <https://orcid.org/0000-0003-4487-5805>
 Hans Schnyder  <https://orcid.org/0000-0002-0139-7535>
 Lisa Wingate  <https://orcid.org/0000-0003-1921-1556>

Data availability

The MuSICA model is written in FORTRAN 90 with scripts in PYTHON or R. The model code is currently on a private repository (https://bitbucket.org/musica_dev/musica/src/master/) accessible upon request and should very soon be moved to a public repository. The data and the R code for the allocation-and-growth model are also available upon request.

References

- Anderson WT, Bernasconi SM, McKenzie JA. 1998. Oxygen and carbon isotopic record of climatic variability in tree ring cellulose (*Picea abies*): An example from central Switzerland (1913–1995). *Journal of Geophysical Research* 103: 31625–31636.
- Baca Cabrera JC, Hirl RT, Zhu J, Schäufele R, Schnyder H. 2020. Atmospheric CO₂ and VPD alter the diel oscillation of leaf elongation in perennial ryegrass: compensation of hydraulic limitation by stored-growth. *New Phytologist* 227: 1776–1789.
- Ball JT, Woodrow IE, Berry JA. 1987. A model predicting stomatal conductance and its contribution to the control of photosynthesis under different environmental conditions. In: Biggins J, ed. *Progress in photosynthesis research*, vol. 4. Dordrecht, the Netherlands: Martinus Nijhoff, 221–224.
- Barbour MM. 2007. Stable oxygen isotope composition of plant tissue: a review. *Functional Plant Biology* 34: 83–94.
- Barbour MM, Cernusak LA, Farquhar GD. 2005. Factors affecting the oxygen isotope ratio of plant organic material. In: Flanagan LB, Ehleringer JR, Pataki DE, eds. *Stable isotopes and biosphere–atmosphere interactions: processes and biological controls*. San Diego, CA, USA: Academic Press, 9–28.
- Barbour MM, Farquhar GD. 2000. Relative humidity- and ABA-induced variation in carbon and oxygen isotope ratios of cotton leaves. *Plant, Cell & Environment* 23: 473–485.
- Barbour MM, Fischer RA, Sayre KD, Farquhar GD. 2000b. Oxygen isotope ratio of leaf and grain material correlates with stomatal conductance and grain yield in irrigated wheat. *Functional Plant Biology* 27: 625–637.

- Barbour MM, Schurr U, Henry BK, Wong SC, Farquhar GD. 2000a. Variation in the oxygen isotope ratio of phloem sap sucrose from castor bean. Evidence in support of the Péclet effect. *Plant Physiology* 123: 671–679.
- Barbour MM, Walcroft AS, Farquhar GD. 2002. Seasonal variation in $\delta^{13}\text{C}$ and $\delta^{18}\text{O}$ of cellulose from growth rings of *Pinus radiata*. *Plant, Cell & Environment* 25: 1483–1499.
- Barnes CJ, Allison GB. 1988. Tracing of water movement in the unsaturated zone using stable isotopes of hydrogen and oxygen. *Journal of Hydrology* 100: 143–176.
- Battipaglia G, Saurer M, Cherubini P, Calfapietra C, McCarthy HR, Norby RJ, Cotrufo MF. 2013. Elevated CO_2 increases tree-level intrinsic water use efficiency: insights from carbon and oxygen isotope analysis in tree rings across three FACE sites. *New Phytologist* 197: 544–554.
- Bowen GJ, Wilkinson B. 2002. Spatial distribution of $\delta^{18}\text{O}$ in meteoric precipitation. *Geology* 30: 315–318.
- Brendel O, Iannetta PPM, Stewart D. 2000. A rapid and simple method to isolate pure alpha-cellulose. *Phytochemical Analysis* 11: 7–10.
- Brinkmann N, Seeger S, Weiler M, Buchmann N, Eugster W, Kahmen A. 2018. Employing stable isotopes to determine the residence times of soil water and the temporal origin of water taken up by *Fagus sylvatica* and *Picea abies* in a temperate forest. *New Phytologist* 219: 1300–1313.
- Cernusak LA, Farquhar GD, Pate JS. 2005. Environmental and physiological controls over oxygen and carbon isotope composition of Tasmanian blue gum, *Eucalyptus globulus*. *Tree Physiology* 25: 129–146.
- Cernusak LA, Wong SC, Farquhar GD. 2003. Oxygen isotope composition of phloem sap in relation to leaf water in *Ricinus communis*. *Functional Plant Biology* 30: 1059–1070.
- Cheesman AW, Cernusak LA. 2017. Infidelity in the outback: climate signal recorded in $\Delta^{18}\text{O}$ of leaf but not branch cellulose of eucalypts across an Australian aridity gradient. *Tree Physiology* 37: 554–564.
- Damesin C, Lelarge C. 2003. Carbon isotope composition of current-year shoots from *Fagus sylvatica* in relation to growth, respiration and use of reserves. *Plant, Cell & Environment* 26: 207–219.
- Dansgaard W. 1964. Stable isotopes in precipitation. *Tellus* 16: 436–468.
- DeNiro MJ, Epstein S. 1979. Relationship between the oxygen isotope ratios of terrestrial plant cellulose, carbon dioxide, and water. *Science* 204: 51–53.
- Durand JL, Onillon B, Schnyder H, Rademacher I. 1995. Drought effects on cellular and spatial parameters of leaf growth in tall fescue. *Journal of Experimental Botany* 46: 1147–1155.
- Farquhar GD, Barbour MM, Henry BK. 1998. Interpretation of oxygen isotope composition of leaf material. In: Griffiths H, ed. *Stable isotopes: integration of biological, ecological and geochemical processes*. Oxford, UK: BIOS Scientific, 27–61.
- Gamnitzer U, Schäufele R, Schnyder H. 2009. Observing ^{13}C labelling kinetics in CO_2 respired by a temperate grassland ecosystem. *New Phytologist* 184: 376–386.
- Gan KS, Wong SC, Yong JWH, Farquhar GD. 2003. Evaluation of models of leaf water ^{18}O enrichment using measurements of spatial patterns of vein xylem water, leaf water and dry matter in maize leaves. *Plant, Cell & Environment* 26: 1479–1495.
- Gangi L, Rothfuss Y, Ogée J, Wingate L, Vereecken H, Brüggemann N. 2015. A new method for in situ measurements of oxygen isotopologues of soil water and carbon dioxide with high time resolution. *Vadose Zone Journal* 14: 10.2136/vzj2014.11.0169.
- Gaudinski JB, Dawson TE, Quideau S, Schuur EAG, Roden JS, Trumbore SE, Sandquist DR, Oh S-W, Wasylishen RE. 2005. Comparative analysis of cellulose preparation techniques for use with ^{13}C , ^{14}C , and ^{18}O isotopic measurements. *Analytical Chemistry* 77: 7212–7224.
- Gessler A, Brandes E, Buchmann N, Helle G, Rennenberg H, Barnard RL. 2009. Tracing carbon and oxygen isotope signals from newly assimilated sugars in the leaves to the tree-ring archive. *Plant, Cell & Environment* 32: 780–795.
- Gessler A, Brandes E, Keitel C, Boda S, Kayler ZE, Granier A, Barbour M, Farquhar GD, Treyde K. 2013. The oxygen isotope enrichment of leaf-exported assimilates – does it always reflect lamina leaf water enrichment? *New Phytologist* 200: 144–157.
- Gessler A, Ferrio JP, Hommel R, Treyde K, Werner RA, Monson RK. 2014. Stable isotopes in tree rings: towards a mechanistic understanding of isotope fractionation and mixing processes from the leaves to the wood. *Tree Physiology* 34: 796–818.
- Gessler A, Peuke AD, Keitel C, Farquhar GD. 2007. Oxygen isotope enrichment of organic matter in *Ricinus communis* during the diel course and as affected by assimilate transport. *New Phytologist* 174: 600–613.
- Grams TEE, Kozovits AR, Häberle K-H, Matyssek R, Dawson TE. 2007. Combining $\delta^{13}\text{C}$ and $\delta^{18}\text{O}$ analyses to unravel competition, CO_2 and O_3 effects on the physiological performance of different-aged trees. *Plant, Cell & Environment* 30: 1023–1034.
- Helliker BR, Ehleringer JR. 2000. Establishing a grassland signature in veins: ^{18}O in the leaf water of C_3 and C_4 grasses. *Proceedings of the National Academy of Sciences, USA* 97: 7894–7898.
- Helliker BR, Ehleringer JR. 2002a. Differential ^{18}O enrichment of leaf cellulose in C_3 versus C_4 grasses. *Functional Plant Biology* 29: 435–442.
- Helliker BR, Ehleringer JR. 2002b. Grass blades as tree rings: environmentally induced changes in the oxygen isotope ratio of cellulose along the length of grass blades. *New Phytologist* 155: 417–424.
- Hemming D, Fritts H, Leavitt SW, Wright W, Long A, Shashkin A. 2001. Modelling tree-ring $\delta^{13}\text{C}$. *Dendrochronologia* 19: 23–38.
- Hill SA, Waterhouse JS, Field EM, Switsur VR, apRees T. 1995. Rapid recycling of triose phosphates in oak stem tissue. *Plant, Cell & Environment* 18: 931–936.
- Hirl RT, Schnyder H, Ostler U, Schäufele R, Schleip I, Vetter S, Auerswald K, Baca Cabrera JC, Wingate L, Barbour MM *et al.* 2019. The ^{18}O ecohdrology of a grassland ecosystem – predictions and observations. *Hydrology and Earth Systems Science* 23: 2581–2600.
- Keel SG, Joos F, Spahni R, Saurer M, Weigt RB, Klesse S. 2016. Simulating oxygen isotope ratios in tree ring cellulose using a dynamic global vegetation model. *Biogeosciences* 13: 3869–3886.
- Kress A, Saurer M, Siegwolf RTW, Frank DC, Esper J, Bugmann H. 2010. A 350 year drought reconstruction from Alpine tree ring stable isotopes. *Global Biogeochemical Cycles* 24: GB2011.
- Lalonde S, Tegeder M, Throne-Holst M, Frommer WB, Patrick JW. 2003. Phloem loading and unloading of sugars and amino acids. *Plant, Cell & Environment* 26: 37–56.
- Lavergne A, Gennaretti F, Risi C, Daux V, Boucher E, Savard MM, Naulier M, Villalba R, Bégin C, Guiot J. 2017. Modelling tree ring cellulose $\delta^{18}\text{O}$ variations in two temperature-sensitive tree species from North and South America. *Climate of the Past* 13: 1515–1526.
- Lehmann MM, Gamarra B, Kahmen A, Siegwolf RTW, Saurer M. 2017. Oxygen isotope fractionations across individual leaf carbohydrates in grass and tree species. *Plant, Cell & Environment* 40: 1658–1670.
- Lemaire G, Da Silva SC, Agnusdei M, Wade M, Hodgson J. 2009. Interactions between leaf lifespan and defoliation frequency in temperate and tropical pastures: a review. *Grass and Forage Science* 64: 341–353.
- Lemaire G, Hodgson J, de Moraes A, Nabinger C, de F Carvalho PC. 2000. *Grassland ecophysiology and grazing ecology*. Wallingford, UK: CABI Publishing.
- Liu HT, Gong XY, Schäufele R, Yang F, Hirl RT, Schmidt A, Schnyder H. 2016. Nitrogen fertilization and $\delta^{18}\text{O}$ of CO_2 have no effect on ^{18}O -enrichment of leaf water and cellulose in *Cleistogenes squarrosa* (C_4) – is VPD the sole control? *Plant, Cell & Environment* 39: 2701–2712.
- Liu HT, Schäufele R, Gong XY, Schnyder H. 2017a. $\delta^{18}\text{O}$ and $\delta^2\text{H}$ of water in the leaf growth-and-differentiation zone of grasses is close to source water in both humid and dry atmospheres. *New Phytologist* 214: 1423–1431.
- Liu HT, Yang F, Gong XY, Schäufele R, Schnyder H. 2017b. An oxygen isotope chronometer for cellulose deposition: the successive leaves formed by tillers of a C_4 perennial grass. *Plant, Cell & Environment* 40: 2121–2132.
- Lötscher M, Klumpp K, Schnyder H. 2004. Growth and maintenance respiration for individual plants in hierarchically structured canopies of *Medicago sativa* and *Helianthus annuus*: the contribution of current and old assimilates. *New Phytologist* 164: 305–316.
- Medlyn BE, Dreyer E, Ellsworth D, Forstreuter M, Harley PC, Kirschbaum MUF, Le Roux X, Montpied P, Strassmeyer J, Walcroft A *et al.* 2002. Temperature response of parameters of a biochemically based model of

- photosynthesis. II. A review of experimental data. *Plant, Cell & Environment* 25: 1167–1179.
- Miner GL, Bauerle WL, Baldocchi DD. 2017. Estimating the sensitivity of stomatal conductance to photosynthesis: a review. *Plant, Cell & Environment* 40: 1214–1238.
- Moreno-Gutiérrez C, Dawson TE, Nicolás E, Querejeta JI. 2012. Isotopes reveal contrasting water use strategies among coexisting plant species in a Mediterranean ecosystem. *New Phytologist* 196: 489–496.
- Ogée J, Barbour MM, Wingate L, Bert D, Bosc A, Stievenard M, Lambrot C, Pierre M, Bariac T, Loustau D *et al.* 2009. A single-substrate model to interpret intra-annual stable isotope signals in tree-ring cellulose. *Plant, Cell & Environment* 32: 1071–1090.
- Ogée J, Brunet Y, Loustau D, Berbigier P, Delzon S. 2003. MuSICA, a CO₂, water and energy multilayer, multi-leaf pine forest model: evaluation from hourly to yearly time scales and sensitivity analysis. *Global Change Biology* 9: 697–717.
- Ostler U, Schleip I, Lattanzi FA, Schnyder H. 2016. Carbon dynamics in aboveground biomass of co-dominant plant species in a temperate grassland ecosystem: same or different? *New Phytologist* 210: 471–484.
- R Core Team. 2017. *R: a language and environment for statistical computing v.3.4.2*. Vienna, Austria: R Foundation for Statistical Computing.
- Roden JS, Ehleringer JR. 1999. Hydrogen and oxygen isotope ratios of tree-ring cellulose for riparian trees grown long-term under hydroponically controlled environments. *Oecologia* 121: 467–477.
- Roden JS, Lin GG, Ehleringer JR. 2000. A mechanistic model for interpretation of hydrogen and oxygen isotope ratios in tree-ring cellulose. *Geochimica et Cosmochimica Acta* 64: 21–35.
- Rogers A, Fischer BU, Bryant J, Frehner M, Blum H, Raines CA, Long SP. 1998. Acclimation of photosynthesis to elevated CO₂ under low-nitrogen nutrition is affected by the capacity for assimilate utilization. Perennial ryegrass under free-air CO₂ enrichment. *Plant Physiology* 118: 683–689.
- Royle J, Ogée J, Wingate L, Hodgson DA, Convey P, Griffiths H. 2013. Temporal separation between CO₂ assimilation and growth? Experimental and theoretical evidence from the desiccation-tolerant moss *Syntrichia ruralis*. *New Phytologist* 197: 1152–1160.
- Saurer M, Schweingruber F, Vaganov EA, Shiyatov SG, Siegwolf R. 2002. Spatial and temporal oxygen isotope trends at the northern tree-line in Eurasia. *Geophysical Research Letters* 29: 10.1029/2001GL013739.
- Scheidegger Y, Saurer M, Bahn M, Siegwolf R. 2000. Linking stable oxygen and carbon isotopes with stomatal conductance and photosynthetic capacity: a conceptual model. *Oecologia* 125: 350–357.
- Schleip I. 2013. *Carbon residence time in above-ground and below-ground biomass of a grazed grassland community*. PhD Thesis. Munich, Germany: Technical University of Munich.
- Schleip I, Lattanzi FA, Schnyder H. 2013. Common leaf life span of co-dominant species in a continuously grazed temperate pasture. *Basic and Applied Ecology* 14: 54–63.
- Schnyder H, Schwertl M, Auerswald K, Schäufele R. 2006. Hair of grazing cattle provides an integrated measure of the effects of site conditions and interannual weather variability on $\delta^{13}\text{C}$ of temperate humid grassland. *Global Change Biology* 12: 1315–1329.
- Song X, Barbour MM, Saurer M, Helliker BR. 2011. Examining the large-scale convergence of photosynthesis-weighted tree leaf temperatures through stable oxygen isotope analysis of multiple data sets. *New Phytologist* 192: 912–924.
- Song X, Farquhar GD, Gessler A, Barbour MM. 2014. Turnover time of the non-structural carbohydrate pool influences $\delta^{18}\text{O}$ of leaf cellulose. *Plant, Cell & Environment* 37: 2500–2507.
- Sternberg LSL, DeNiro MJ, Savidge RA. 1986. Oxygen isotope exchange between metabolites and water during biochemical reactions leading to cellulose synthesis. *Plant Physiology* 82: 423–427.
- Sternberg L, Ellsworth PFV. 2011. Divergent biochemical fractionation, not convergent temperature, explains cellulose oxygen isotope enrichment across latitudes. *PLoS ONE* 6: e28040.
- Sullivan PF, Welker JM. 2007. Variation in leaf physiology of *Salix arctica* within and across ecosystems in the High Arctic: test of a dual isotope ($\Delta^{13}\text{C}$ and $\Delta^{18}\text{O}$) conceptual model. *Oecologia* 151: 372–386.
- Szejner P, Clute T, Anderson E, Evans MN, Hu J. 2020. Reduction in lumen area is associated with the $\delta^{18}\text{O}$ exchange between sugars and source water during cellulose synthesis. *New Phytologist* 226: 1583–1593.
- Thornley JHM. 1998. *Grassland dynamics: an ecosystem simulation model*. Wallingford, UK: CAB International.
- Thornley JHM, Cannell MGR. 2000. Modelling the components of plant respiration: representation and realism. *Annals of Botany* 85: 55–67.
- Tjoelker MG, Oleksyn J, Reich PB. 2001. Modelling respiration of vegetation: evidence for a general temperature-dependent Q_{10} . *Global Change Biology* 7: 223–230.
- Verbancic J, Lunn JE, Stitt M, Persson S. 2018. Carbon supply and the regulation of cell wall synthesis. *Molecular Plant* 11: 75–94.
- Willmott CJ, Matsuura K. 2005. Advantages of the mean absolute error (MAE) over the root mean square error (RMSE) in assessing average model performance. *Climate Research* 30: 79–82.
- Wingate L, Ogée J, Burrell R, Bosc A, Devaux M, Grace J, Loustau D, Gessler A. 2010. Photosynthetic carbon isotope discrimination and its relationship to the carbon isotope signals of stem, soil and ecosystem respiration. *New Phytologist* 188: 576–589.
- Wohlfahrt G, Bahn M, Horak I, Tappeiner U, Cernusca A. 1998. A nitrogen sensitive model of leaf carbon dioxide and water vapour gas exchange: application to 13 key species from differently managed mountain grassland ecosystems. *Ecological Modelling* 113: 179–199.
- Yoshimura K, Frankenberg C, Lee J, Kanamitsu M, Worden J, Rockmann T. 2011. Comparison of an isotopic atmospheric general circulation model with new quasi-global satellite measurements of water vapor isotopologues. *Journal of Geophysical Research* 116: D19118.

Supporting Information

Additional Supporting Information may be found online in the Supporting Information section at the end of the article.

Fig. S1 Sensitivity of modelled $\delta^{18}\text{O}_{\text{cellulose}}$ and $\Delta^{18}\text{O}_{\text{cellulose}}$ to the parameters of the allocation-and-growth model, to the responsiveness parameter of the Ball–Woodrow–Berry stomatal conductance model (m_{gs} ; Ball *et al.*, 1987), to maximum rate of carboxylation and potential rate of electron transport (V_{cmax} and J_{max}), and to incoming short-wave radiation and wind speed.

Fig. S2 Relationship between the $\delta^{18}\text{O}$ of rain collected at the Grünschwaige study site (see Hirl *et al.*, 2019) and plant-available water and air temperature.

Fig. S3 Plot of $\Delta^{18}\text{O}_{\text{cellulose}}$ vs midday mean relative humidity and daily mean air temperature.

Fig. S4 Sensitivity of $\Delta^{18}\text{O}_{\text{cellulose}}$ to air temperature, predicted based on a constant ($\epsilon_{\text{bio}} = 27\text{‰}$) or temperature-sensitive biochemical fractionation.

Fig. S5 Relationship between p_{ex} and the mean residence time of the metabolic pool ($\tau_{\text{pool,out}}$), both averaged over the integration time (400 GDD).

Fig. S6 Boxplots showing the effect of plant-available water on observed $\Delta^{18}\text{O}_{\text{cellulose}}$, predicted $\Delta^{18}\text{O}_{\text{cellulose}}$ and modelled midday canopy conductance, g_{canopy} .

Methods S1 The MuSICA model.

Methods S2 The allocation-and-growth model.

Methods S3 Derivation of the $p_{ex}p_x$ -RH function for the standard simulation.

Table S1 Correlation between meteorological variables.

Please note: Wiley Blackwell are not responsible for the content or functionality of any Supporting Information supplied by the authors. Any queries (other than missing material) should be directed to the *New Phytologist* Central Office.



About *New Phytologist*

- *New Phytologist* is an electronic (online-only) journal owned by the New Phytologist Foundation, a **not-for-profit organization** dedicated to the promotion of plant science, facilitating projects from symposia to free access for our Tansley reviews and Tansley insights.
- Regular papers, Letters, Research reviews, Rapid reports and both Modelling/Theory and Methods papers are encouraged. We are committed to rapid processing, from online submission through to publication 'as ready' via *Early View* – our average time to decision is <26 days. There are **no page or colour charges** and a PDF version will be provided for each article.
- The journal is available online at Wiley Online Library. Visit **www.newphytologist.com** to search the articles and register for table of contents email alerts.
- If you have any questions, do get in touch with Central Office (np-centraloffice@lancaster.ac.uk) or, if it is more convenient, our USA Office (np-usaoffice@lancaster.ac.uk)
- For submission instructions, subscription and all the latest information visit **www.newphytologist.com**